
Learning from Time Series under Temporal Label Noise

Sujay Nagaraj^{1 2} Walter Gerych³ Sana Tonekaboni^{1 2} Anna Goldenberg^{1 2 4 5} Berk Ustun⁶
Thomas Hartvigsen⁷

Abstract

Many sequential classification tasks are affected by *label noise* that varies over time. Such noise can cause label quality to improve, worsen, or periodically change over time. We first propose and formalize *temporal label noise*, an unstudied problem for sequential classification of time series. In this setting, multiple labels are recorded in sequence while being corrupted by a time-dependent noise function. We first demonstrate the importance of modelling the temporal nature of the label noise function and how existing methods will consistently underperform. We then propose methods that can train noise-tolerant classifiers by estimating the temporal label noise function directly from data. We show that our methods lead to state-of-the-art performance in the presence of diverse temporal label noise functions using real and synthetic data.

1. Introduction

Many supervised learning datasets contain *noisy* observations of ground truth labels. Such *label noise* can arise due to issues in human annotation or data collection [1, 26], including lack of expertise among annotators [28, 72], discrepancies in labelling difficulty [13, 27, 72], subjective labeling tasks [42, 50, 55], and systematic issues in automatic annotation like measurement error [29, 46].

Label noise is a key vulnerability of modern supervised learning [18, 23, 70]. Intuitively, models trained with noisy labels may learn to predict noise rather than the ground truth. Such models will then underperform at test time when they must instead predict the ground truth. This problem is exacerbated by deep learning methods, which have the representational capacity to overfit the noise [2, 15, 16, 36].

¹University of Toronto ²Vector Institute ³Massachusetts Institute of Technology ⁴The Hospital for Sick Children ⁵CIFAR ⁶University of California, San Diego ⁷University of Virginia. Correspondence to: Sujay Nagaraj <s.nagaraj@mail.utoronto.ca>.

While there are many methods designed to be robust to label noise, they are all designed for *static*, time-invariant data [4, 38, 40, 60]. Real-world problems (e.g., healthcare) often involve time series data, where multiple labels are collected over time. Labels typically represent the change in underlying states over time - for example an individual transitioning in and out of testing positive for COVID-19. As these labels are generated over time, *label noise* can surely change over time. Existing approaches are ill-equipped to handle this phenomenon. Here, we introduce the concept of *temporal label noise*. We argue that accounting for temporal label noise can lead to time series models robust to noise. To the best of our knowledge, learning from temporal label noise is unstudied, yet exists in a range of tasks. For example:

Longitudinal Self-Reporting for Mental Health: Mental health studies often collect self-reported survey data over long periods of time. Such self-reporting is known to be biased [6, 47, 49, 66], where participants are more or less likely to report certain features. For example, the accuracy of self-reported alcohol consumption is often seasonal [8].

Human Activity Recognition. Wearable device studies often ask participants to annotate their activities over time. But participants may mislabel due to recall bias, time of day, or labelling-at-random for monetized studies [25, 54].

Clinical Measurement Error: The labels used to train clinical prediction models are often derived from clinician notes in electronic health records. These labels may capture noisier annotations during busy periods, when a patient is deteriorating, or the bedside situation is more chaotic [71].

Classifying time series with temporal label noise is challenging. First, existing losses that are robust to static label noise [41, 43] underperform when facing temporal noise—as we show in our experiments. This means that classifiers can still suffer, even for known temporal noise functions. Worse yet, the temporal label noise function is generally *not* known. Often times, all that is available is a dataset with temporally noisy labels with no indication of which instances or time-steps are more likely to be correct.

We propose novel time series classification objectives which *learn* the temporal noise function from the data. These methods leverage temporal loss functions, which we prove

Our code is available on [GitHub](#).

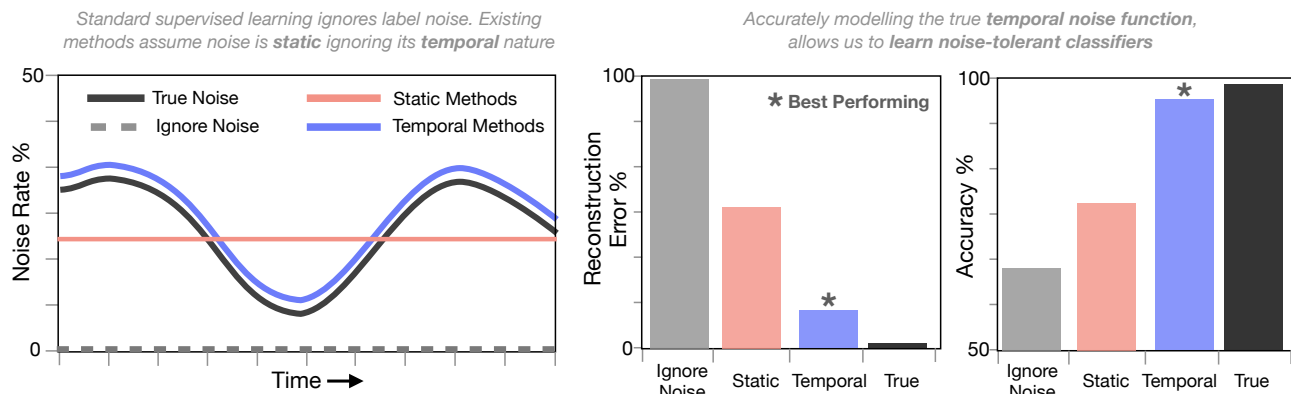


Figure 1: Label quality can vary over time due to *temporal* label noise. Existing methods assume noise is time-invariant (*static*) leading to loss in performance. By accurately modeling temporal label noise, we can improve performance and outperform existing approaches. Here, we show performance improvements on *synth* dataset comparing reconstruction error and accuracy between static and temporal methods subject to 30% temporal label noise (see Appendix E for details).

are *robust to temporal label noise*. These methods can be used out of the box and allow practitioners to learn noise-tolerant time series classifiers, even with unknown, temporal label noise.

Our contributions are as follows:

1. We formalize the problem of learning from noisy labels in temporal settings. We are the first to study this important problem on which we show that prior works under-perform.
2. We propose two loss functions for training models that are robust to temporal label noise. On their own, each can be used to improve prior methods.
3. We propose TENOR, the first method for learning temporal noise functions. By pairing a neural network with our proposed loss functions, TENOR can model any noise function and thereby lead to better classifiers.
4. Our experiments identify that existing methods under-perform in the presence of temporal noise, while our proposed methods lead to better classifiers. This highlights the necessity of accounting for temporal noise.

Related Work

Time Series Machine learning for time series, especially in healthcare, often relies on combining autoregressive approaches to modelling sequences with deep neural network based methods [11, 34, 58]. Primarily in the context of sequence-to-sequence modelling, Recurrent Neural Networks (RNNs) and state space models have gained attention for their ability to model observed data as emanations from underlying latent states that evolve over time. Attention-based mechanisms have further enabled models to prioritize relevant segments of data [65], thereby enhancing performance in tasks such as patient outcome prediction and

treatment optimization [14, 30, 57, 61, 68, 78]. These approaches primarily rely on supervised learning to model changes in latent states over time. In healthcare for example, underlying latent states can be understood as clinical labels (i.e: sick vs healthy) that patients can transition in and out of. An understudied area in this domain is label noise - what happens when the labels we use to learn time series models are corrupted?

Label Noise Our work identifies and addresses gaps in the literature on noisy labels [4, 38, 40, 60]. Prior to this, the vast majority of work on noisy labels has focused on static classification tasks, where label noise cannot change over time. We instead consider a setting in which label noise arises over time, and where the noise rates can therefore change over time. While a few methods have considered noise in time series data [3, 12], they focus on tools to identify individual noisy samples rather than developing general-purpose methods robust to temporal label noise. These studies also suggest that noisy samples can be identified because neighboring time points are unlikely to be corrupted together. However, we propose that neighboring time points are *more* likely to be corrupted together when they were labelled together.

We present a way to learn via empirical risk minimization with *noise-robust loss functions* [20, 33, 38, 41, 69]. Many approaches in the static setting utilize methods for identifying correctly-labeled instances [22, 77], or regularization techniques to minimize the impact of incorrect label [24, 36]. Our results highlight the potential to learn from noisy labels when we have knowledge of the underlying noise process [c.f., 41, 43]. We also develop methods to fit the noise model directly from noisy data [see e.g., 32, 33, 43, 73, 75, 79].

2. Framework

Preliminaries We consider a sequential classification task over C classes and T time steps. Each instance is characterized by a triplet of *sequences* over T time steps $(\mathbf{x}_{1:T}, \mathbf{y}_{1:T}, \tilde{\mathbf{y}}_{1:T}) \in \mathcal{X} \times \mathcal{Y} \times \mathcal{Y}$. Where $\mathcal{X} \subseteq \mathbb{R}^{d \times T}$ and $\mathcal{Y} = \{1, \dots, C\}^T$. Here, $\mathbf{x}_{1:T}$, $\mathbf{y}_{1:T}$, and $\tilde{\mathbf{y}}_{1:T}$ are sequences of instances, *clean labels* and *noisy labels*, respectively.

When learning under temporal label noise, we do not observe the *true* label sequence $\mathbf{y}_{1:T}$. Thus, we only have access to a set of n instances $D = \{(\mathbf{x}_{1:T}, \tilde{\mathbf{y}}_{1:T})_i\}_{i=1}^n$. We assume that the sequences for each instance are generated i.i.d. from a joint distribution $P_{\mathbf{x}_{1:T}, \mathbf{y}_{1:T}, \tilde{\mathbf{y}}_{1:T}}$, where the label noise process can vary over time. This distribution obeys two standard assumptions in sequential modeling and label noise [5, 10, 62]:

Assumption 1 (Markov Assumption). *A label at time t depends only on the sequence of feature vectors up to t :*

$$p(\mathbf{y}_{1:T} | \mathbf{x}_{1:T}) = \prod_{t=1}^T p(y_t | \mathbf{x}_{1:t})$$

Assumption 2 (Feature-Independence). *The sequence of noisy labels is conditionally independent of the features given the true labels: $\tilde{y}_{1:t} \perp\!\!\!\perp \mathbf{x}_{1:t} | \mathbf{y}_{1:t}$ for $t = 1, \dots, T$*

Assumption 1 allows us to elegantly factorize the joint distribution of a sequence: $p(\tilde{\mathbf{y}}_{1:T} | \mathbf{x}_{1:T}) = \prod_{t=1}^T q_t(\tilde{y}_t | \mathbf{x}_{1:t})$. Assumption 2 allows for the noisy label distribution at t to be further decomposed as:

$$q_t(\tilde{y}_t | \mathbf{x}_{1:t}) = \sum_{y \in \mathcal{Y}} q_t(\tilde{y}_t | y_t = y) p(y_t = y | \mathbf{x}_{1:t}) \quad (1)$$

2.1. Learning from Temporal Label Noise

Our goal is to learn a sequential classification model $\mathbf{h}_\theta : \mathcal{X} \rightarrow \mathbb{R}^C$ with model parameters $\theta \in \Theta$. Here, $\mathbf{h}_\theta(\mathbf{x}_{1:t})$ returns an estimate of $p(\mathbf{y}_t | \mathbf{x}_{1:t})$. To infer the label at time step t , \mathbf{h}_θ takes as input a sequence of feature vectors up to t , and outputs a sequence of labels by taking the arg max of the predicted distribution for each time step (see e.g., [5, 62]).

We estimate parameters $\hat{\theta}$ for a model robust to noise, by maximizing the expected accuracy as measured in terms of the *clean* labels:

$$\hat{\theta} = \operatorname{argmax}_{\theta \in \Theta} \mathbb{E}_{\mathbf{y}_{1:T} | \mathbf{x}_{1:T}} \prod_{t=1}^T p(y_t = \mathbf{h}_\theta(\mathbf{x}_{1:t}) | \mathbf{x}_{1:t})$$

However, during training time we only have access to sequences of *noisy* labels. To demonstrate how we can sidestep this limitation, we first need to introduce a flexible

way to model sequential noisy labels. Existing methods assume that noise is time-invariant (Fig. 1). To relax this assumption, we capture the temporal nature of noisy labels using a *temporal label noise function*, in Def. 1.

Definition 1. Given a sequential classification task with C classes and noisy labels, the *temporal label noise function* is a matrix-valued function $\mathbf{Q} : \mathbb{R}_+ \rightarrow [0, 1]^{C \times C}$ that specifies the label noise distribution at any time $t > 0$.

We denote the output of the temporal noise function at time t as $\mathbf{Q}_t := \mathbf{Q}(t)$. This is a $C \times C$ matrix whose i, j^{th} entry encodes the flipping probability of observing a noisy label j given clean label i at time t : $q_t(\tilde{y}_t = j | y_t = i)$. We observe that \mathbf{Q}_t is positive, row-stochastic, and diagonally dominant — ensuring that \mathbf{Q}_t encodes a valid probability distribution [33, 43].

\mathbf{Q}_ω denotes a temporal noise function parameterized by a function with parameters ω . This parameterization can be constructed to encode essentially any temporal noise function. As shown in Table 1, we can capture a wide variety of temporal noise in time series classification tasks using this representation.

2.2. Loss Correction

Modeling temporal label noise is the first piece of the puzzle in training time series classifiers robust to label noise. However, we still need to consider how to leverage these noise models during empirical risk minimization. It remains unclear if and how existing loss correction techniques work for time series. Here we present theoretical results showing that learning is possible in our setting when we know the true temporal noise function $\mathbf{Q}(t)$. We include proofs in Appendix A.

We begin by treating the noisy posterior as the matrix-vector product of a noise transition matrix and a clean class posterior (Eq. (1)). To this effect, we define the *forward sequence loss*:

Definition 2. Given a sequential classification task over T time steps, a noise function $\mathbf{Q}(t)$, and a proper composite loss function ¹ ℓ_t , the *forward sequence loss* of a model \mathbf{h}_θ on an instance $(\tilde{\mathbf{y}}_{1:T}, \mathbf{x}_{1:T})$:

$$\vec{\ell}_{seq}(\tilde{\mathbf{y}}_{1:T}, \mathbf{x}_{1:T}, \mathbf{h}_\theta) := \sum_{t=1}^T \ell_t(\tilde{y}_t, \mathbf{Q}_t^\top \mathbf{h}_\theta(\mathbf{x}_{1:t}))$$

An intriguing property of the *forward sequence loss* is that the minimizer of the *forward sequence loss* over the noisy labels maximizes the likelihood of the data over the clean

¹A loss that is well-calibrated for probability estimation (e.g., NLL loss) and incorporates a link function mapping model outputs to probability estimates (see [51] for more detail)

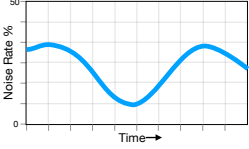
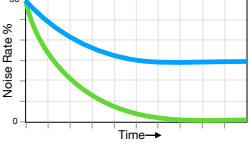
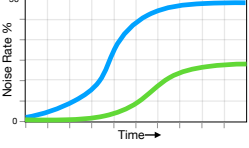
Pattern	Depiction	Noise Model – Q_{ij}	Parameters	Applications
Periodic		$\frac{1}{2} + \frac{1}{2} \sin(\alpha_{ij}t + \phi_{ij})$	$\omega_{ij} = (\alpha_{ij}, \phi_{ij})$ α controls frequency ϕ controls shift	Annotation reliability varies over time of day – e.g., due to changes in annotator attentiveness over the day [17].
Decay		$\alpha_{ij} \exp(-\beta_{ij}t)$	$\omega_{ij} = (\alpha_{ij}, \lambda_{ij})$ α controls initial noise β controls decay rate	Annotation reliability improves rapidly (e.g., diagnostic accuracy of COVID-19 rapidly improved at the onset of the pandemic [44]) or improves and plateaus (e.g., irreducible uncertainty in labels [48])
Growth		$\frac{\alpha_{ij}}{1 + \exp(-\beta_{ij}(t - \gamma_{ij}))}$	$\omega_{ij} = (\alpha_{ij}, \beta_{ij}, \gamma_{ij})$ α controls limit β controls growth rate γ controls inflection point	Annotation reliability decreases abruptly – e.g., due to rapid adoption of improved clinical guidelines [59]. Or, it decreases gradually – e.g., due to underdiagnosis during the pandemic due to healthcare disruptions [19]

Table 1: Overview of noise functions for time series classification tasks. We show the noise model $Q(t)$ and parameters ω needed to model $q(\tilde{y}_t = j | y_t = i)$. Practitioners can model for label noise by choosing a parametric class to capture effects and fit parametric representations from data. The choice of noise model can differ across classes and subgroups (see the *Mixed* model in Section 4). We include other models and details in Appendix D.

labels. This suggests that the *forward sequence loss* is robust to label noise:

Theorem 1. *A classifier that minimizes the empirical forward sequence loss over the noisy labels maximizes the empirical likelihood of the data over the clean labels.*

$$\begin{aligned} & \operatorname{argmin}_{\theta \in \Theta} \mathbb{E}_{\tilde{\mathbf{y}}_{1:T}, \mathbf{x}_{1:T}} \overleftarrow{\ell}_{seq}(\tilde{\mathbf{y}}_{1:T}, \mathbf{x}_{1:T}, \mathbf{h}_{\theta}) \\ &= \operatorname{argmin}_{\theta \in \Theta} \sum_{t=1}^T \mathbb{E}_{\mathbf{y}_{1:t}, \mathbf{x}_{1:t}} \ell_t(y_t, \mathbf{h}_{\theta}(\mathbf{x}_{1:t})) \end{aligned}$$

An alternative strategy is the *backward sequence loss*, which extends the backward loss of Patrini et al. [43] to a temporal setting:

Definition 3. Given a sequential classification task over T time steps, a noise function $Q(t)$, the *backward sequence loss* of \mathbf{h}_{θ} on an instance $(\tilde{\mathbf{y}}_{1:T}, \mathbf{x}_{1:T})$ is:

$$\overleftarrow{\ell}_{seq}(\tilde{\mathbf{y}}_{1:T}, \mathbf{x}_{1:T}, \mathbf{h}_{\theta}) := \sum_{t=1}^T \overleftarrow{\ell}_t(\tilde{y}_t, \mathbf{h}_{\theta}(\mathbf{x}_{1:t})).$$

Here $\overleftarrow{\ell}_t(c, \mathbf{h}_{\theta}(\mathbf{x}_{1:t})) = [Q_t^{-1}]_{c,:} \cdot \ell(\mathbf{h}_{\theta}(\mathbf{x}_{1:t}))$ and $\ell(\mathbf{h}_{\theta}(\mathbf{x}_{1:t})) := [\ell(c, \mathbf{h}_{\theta}(\mathbf{x}_{1:t}))]_{c=1:C}^{\top}$ is a vector containing the negative log-likelihood loss of $\ell(c, \mathbf{h}_{\theta}(\mathbf{x}_{1:t}))$ for observed class c .

Intuitively, the term “backward” reflects the fact that the function corrects for label noise by using the noise model and the noisy labels to infer the clean labels. In Theorem 2, we show that we can maximize accuracy on the clean labels using only noisy labels with the *backward sequence loss*:

Theorem 2. *Minimizing the expected backward sequence loss over noisy label sequences maximizes the joint likelihood over clean label sequences.*

$$\begin{aligned} & \operatorname{argmax}_{\theta \in \Theta} \mathbb{E}_{\mathbf{y}_{1:T} | \mathbf{x}_{1:T}} \log(p_{\theta}(\mathbf{y}_{1:T} | \mathbf{x}_{1:T})) \\ &= \operatorname{argmin}_{\theta \in \Theta} \mathbb{E}_{\tilde{\mathbf{y}}_{1:T} | \mathbf{x}_{1:T}} \overleftarrow{\ell}_{seq}(\mathbf{h}_{\theta}(\mathbf{x}_{1:T})) \end{aligned}$$

Both theorems imply that we can *train on the noisy distribution* and learn a noise-tolerant classifier in expectation. Though both loss functions provide this guarantee, the *backward sequence loss* requires a costly and potentially numerically unstable matrix-inversion at *every* time step. This can be especially problematic when C and T are large. More importantly, we find that the *backward sequence loss* performs *substantially* worse than *forward sequence loss* in practice (e.g., see Section 4.2 for Analysis). For these reasons, we utilize the *forward sequence loss* in subsequent sections.

3. Methods

We have shown how to leverage the temporal label noise function to train models robust to noise. However, the label noise function is generally not available *a priori* and should ideally be estimated from data. In this section we propose methods for *learning* the temporal noise function from noisy data alone. We present a number of methods for different use cases, including: joint methods, which learn the model and temporal noise function in a single-step procedure; as well as a plug-in approach, which first estimates the temporal noise function and “plugs in” to a loss correction method.

Finally, we discuss practical considerations when choosing between them.

3.1. Joint Continuous Estimation

We start with a method that can simultaneously learn a time series classifier and the temporal noise function. Given a noisy dataset, we learn these elements by solving for $t = 1, \dots, T$ an optimization problem of the form:

$$\begin{aligned} \min_{\omega, \theta} \quad & \text{Vol}(\mathbf{Q}_\omega(t)) \\ \text{s.t.} \quad & \mathbf{Q}_\omega(t)^\top \mathbf{h}_\theta(\mathbf{x}_{1:t}) = p(\tilde{y}_t | \mathbf{x}_{1:t}) \end{aligned} \quad (2)$$

This objective, which we refer to as the **Temporal Noise Robust** objective (TENOR), is designed to return a faithful representation of the noise function $\hat{\omega}$ by imposing the *minimum-volume simplex* assumption [33], and a noise-tolerant sequential classifier $\hat{\theta}$ by minimizing the *forward sequence loss* in Def. 2.

Here, the objective minimizes the volume of the noise matrix, denoted as $\text{Vol}(\mathbf{Q}_t)$. This returns a matrix \mathbf{Q}_t , at each time step, that obeys the *minimum-volume simplex* assumption, which is a standard condition used to ensure identifiability in static classification tasks [see e.g., 33, 76]. In practice, the minimum-volume simple assumption ensures that \mathbf{Q}_t encloses the noisy conditional data distribution at time t : $p(\tilde{y}_t | \mathbf{x}_{1:t})$. Here containment ensures that the estimated noise matrix could have generated each point in the noisy dataset – i.e., so that the corresponding noisy probabilities $p(\tilde{y}_t | \mathbf{x}_{1:t})$ obey Eq. (1). Our use of this assumption guarantees the identifiability of \mathbf{Q}_t when the posterior distribution is sufficiently-scattered over the unit simplex [see also 33, for details].

Implementation The formulation above applies to any generic matrix-valued function according to Def. 1 with parameters ω . Because time series classification tasks can admit many types of temporal label noise functions (Table 1), we must ensure ω has sufficient representational capacity to handle many noise functions. Therefore in practice, we instantiate our solution as a fully connected neural network with parameters ω , $\mathbf{Q}_\omega(\cdot) : \mathbb{R} \rightarrow [0, 1]^{c \times c}$, adjusted to meet Def. 1 (see Appendix D.2).

We can now model any temporal label noise function owing to the universal approximation properties of neural networks. Provided the function space Θ defines autoregressive models of the form $p(y_t | \mathbf{x}_{1:t})$ (e.g., RNNs, Transformers, etc.), we can solve Eq. (2) using an augmented Lagrangian method for equality-constrained optimization problems [7]:

$$\mathcal{L}(\theta, \omega) = \frac{1}{T} \sum_{t=1}^T \left[\|\mathbf{Q}_\omega(t)\|_F + \lambda R_t(\theta, \omega) + \frac{c}{2} |R_t(\theta, \omega)|^2 \right] \quad (3)$$

Here: $\|\mathbf{Q}_\omega(t)\|_F$ denotes the Frobenius norm of $\mathbf{Q}_\omega(t)$, which acts as a convex surrogate for $\text{Vol}(\mathbf{Q}_\omega(t))$. Likewise, $R_t(\theta, \omega) = \frac{1}{n} \sum_{i=1}^n \ell_t(y_{t,i}, \mathbf{Q}_\omega(t)^\top \mathbf{h}_\theta(\mathbf{x}_{1:t,i}))$ denotes the violation of the equality constraint for each $t = 1 \dots T$. $\lambda \in \mathbb{R}_+$ is the Lagrange multiplier and $c > 0$ is a penalty parameter. Both are initially set to a default value of 1, we gradually increase the penalty parameter until the constraint holds and λ converges to the Lagrangian multiplier of Eq. (2) [7]. This approach recovers the best-fit parameters to the optimization problem in Eq. (2). Additional details on our implementation can be found in Appendix C.

3.2. Joint Discontinuous Estimation

An alternative strategy to learning the noise function, is to assume that there is no temporal relationship between each \mathbf{Q}_t across time and treat each time step independently. This is realistic in situations where time steps are unevenly spaced or there are long periods of time between subsequent labels (e.g., some clinical data involves labels collected over years or decades). We can carry out this *discontinuous* estimation by adopting a similar objective as above. Denoting $R_t(\theta) = \frac{1}{n} \sum_{i=1}^n \ell_t(y_{t,i}, \hat{\mathbf{Q}}_t^\top \mathbf{h}_\theta(\mathbf{x}_{1:t,i}))$:

$$\mathcal{L}(\theta, [\hat{\mathbf{Q}}_t]_{t=1}^T) = \frac{1}{T} \sum_{t=1}^T \left[R_t(\theta) + \lambda \cdot \log \det(\hat{\mathbf{Q}}_t) \right] \quad (4)$$

The objective in Eq. (4), denoted as VolMinTime , minimizes the volume of \mathbf{Q} using the log det of a square matrix [33]. In contrast to Eq. (3), each $\hat{\mathbf{Q}}_t$ is parameterized with a *separate* set of trainable real-valued weights, which are learned independently with the data from time t using a standard convex optimization algorithm (e.g., gradient descent). This provides a direct time-series modification of a state-of-the-art technique for noise transition matrix estimation in the static setting [33].

3.3. Plug-In Estimation

It is also advantageous to have a simple, plug-in estimator of the temporal noise function. Plug-in estimators are model-agnostic, can flexibly be deployed to other models, and can be efficient to estimate. We can construct a plug-in estimator of temporal label noise using *anchor points*, instances whose labels are known to be correct. Empirical estimates of the class probabilities of anchor points can be used to estimate the noise function. This estimate can then be plugged into any of the aforementioned loss correction methods in Section 3. Formally, in a sequential setting, anchor points [37, 43, 73] are instances that maximize the probability of belonging to class i at time step t :

$$\bar{\mathbf{x}}_t^i = \arg \max_{\mathbf{x}_t} p(\tilde{y}_t = i | \mathbf{x}_{1:t}) \quad (5)$$

Since $p(y_t = i \mid \bar{x}_{1:t}^i) \approx 1$ for the clean label, we can express each entry of the label noise matrix as:

$$\hat{Q}(t)_{i,j} = p(\tilde{y}_t = j \mid \bar{x}_{1:t}^i). \quad (6)$$

We can use a two-step approach to get a plug-in estimate of $\hat{Q}(t)$. We denote this approach as AnchorTime, where we identify anchor points for each class $y \in \mathcal{Y}$ and $t = 1, \dots, T$ and set each entry of $\hat{Q}(t)_{i,j}$ according to Eq. (6) (see Appendix B for details). This is analogous to the approach in static prediction tasks by Patrini et al. [43].

3.4. Discussion

All three methods improve performance in sequential classification tasks by accounting for temporal label noise (see e.g., Fig. 1 and Section 4). However, they each have their own strengths and limitations. Here we provide practical guidance for users to discriminate between methods:

- Joint Continuous Estimation (TENOR) imposes continuity across time steps – assuming that nearby points likely have similar noise levels. This assumption can improve reconstruction, and thus performance, in settings with multiple time steps as it reduces the effective number of model parameters. Conversely, it may also lead to misspecification in settings that exhibit discontinuity.
- Joint Discontinuous Estimation (VolMinTime) can handle discontinuous temporal noise processes, but requires fitting more parameters, which scales according to T – this can lead to computational challenges and overfitting, especially for long sequences.
- Plug-In estimation (AnchorTime) has a simpler optimization problem. This is useful in cases where separate datasets are used to estimate the noise and to learn the classifier. However, the existence of anchor points is difficult to verify [73].

4. Experiments

We benchmark our methods on a collection of sequential classification tasks from real-world applications. Our goal is to evaluate methods in terms of how robust they are to temporal label noise, and characterize when it is actually important to consider such noise. We provide additional details on our setup and results in Appendix D.

4.1. Setup

Datasets We use four real-world (binary and multiclass) datasets from healthcare, each representing a time-series classification task with sequential labels over a complex feature space that is likely to exhibit temporal label noise. These datasets include sequential accelerometer data for human activity recognition (`har` [52], `har70` [39]) and

continuous EEG signals for sleep detection (`eeg_sleep` [21]) and blink detection (`eeg_eye` [53]). Refer to Appendix D for more details.

To study our approach under the exact data-generating assumptions (Assumption 1 and 2), we also consider a synthetic dataset, `synth`. Synthetic data allows us to confidently identify the causes of variance in model performance. All datasets were treated as binary classification tasks. We also include multiclass results for `eeg_sleep`, `har`, and `synth` in Appendix E.7.

Noise Models We consider labels in the training sample as “ground truth” clean labels and corrupt them using one of five different temporal label noise functions as well as a time-independent function at various noise levels. Three functions are shown in Fig. 2, and complete descriptions are provided in Appendix D.4.

Methods We highlight the key differences between TENOR and existing approaches by training a sequential classifier for each dataset using different Algorithms grouped as follows:

Static. We consider an Uncorrected learning baseline (NLL loss), which assumes no noise exists and two *static* methods: Anchor [37, 43, 73] and VolMinNet [33].

Temporal. We consider TENOR and temporal variations of the static methods that we develop as described in Section 3. We refer to these as AnchorTime, VolMinTime, respectively.

For each dataset, we fit a RNN with *Gated Recurrent Units* (GRU) [9], which is often used in classifying sequential labels [45, 35]. TENOR uses an additional fully-connected neural network with 10 hidden layers to estimate $Q(t)$. Additional details on network architecture are in Appendix D.2.

Evaluation We split each dataset into a *noisy* training sample (80%, used to train the models and correct for label noise) and a *clean* test sample (20%, used to compute unbiased estimates of out-of-sample performance). We evaluate each model in terms of the *test accuracy* on test data and characterize how well each method learns the temporal noise function, using the *Mean Absolute Error* $MAE(Q_t, \hat{Q}_t) := \frac{1}{T} \sum_{t=1}^T \|Q_t - \hat{Q}_t\|$ between the true Q_t and estimated \hat{Q}_t for all t .

4.2. Results and Discussion

In this section, we study the effects of temporal noise when learning models that are more robust to label noise.

Modeling Temporal Noise Improves Performance First, we show clear value in accounting for temporal label noise.

Learning from Time Series under Temporal Label Noise

		synth		har		har70		eeg_eye		eeg_sleep	
		Accuracy \uparrow	MAE \downarrow	Accuracy \uparrow	MAE \downarrow	Accuracy \uparrow	MAE \downarrow	Accuracy \uparrow	MAE \downarrow	Accuracy \uparrow	MAE \downarrow
Static	Uncorrected	79.2 \pm 1.2	–	70.6 \pm 3.0	–	77.3 \pm 1.7	–	71.3 \pm .8	–	68.2 \pm 2.0	–
	Anchor	80.8 \pm 0.7	.16 \pm .00	79.1 \pm 2.6	.13 \pm .01	79.3 \pm .01	.11 \pm .01	75.1 \pm 1.1	.10 \pm .01	65.9 \pm 2.3	.11 \pm .00
	VolMinNet	85.6 \pm 0.9	.10 \pm .00	85.1 \pm 2.7	.11 \pm .00	81.0 \pm 0.7	.11 \pm .00	73.2 \pm 1.4	.13 \pm .00	70.3 \pm 2.2	.11 \pm .00
Temporal	AnchorTime	85.3 \pm 0.8	.10 \pm .01	80.0 \pm 1.8	.11 \pm .01	81.2 \pm 1.1	.08 \pm .00	79.5 \pm 1.8	.06 \pm .01	70.4 \pm 2.8	.06 \pm .00
	VolMinTime	85.8 \pm 0.5	.08 \pm .00	82.4 \pm 2.7	.10 \pm .00	82.0 \pm 1.2	.08 \pm .00	76.9 \pm 1.8	.08 \pm .00	70.3 \pm 3.9	.09 \pm .01
	TENOR	94.4 \pm 1.0	.03 \pm .01	95.8 \pm 2.2	.03 \pm .01	89.0 \pm 0.3	.02 \pm .00	83.7 \pm 0.5	.01 \pm .00	70.4 \pm 2.3	.04 \pm .01

Table 2: Clean test set accuracy (%) and reconstruction error MAE($\hat{Q}(t)$) for all methods and datasets with 30% label noise on average. We report the mean value \pm st.dev for each metric over 10 runs and highlight methods that achieve the best results in **green**. As shown, TENOR achieves superior performance to all baselines. We show results for *Mixed* noise function, which denotes class-conditional noise where one class has increasing noise and one class has decreasing noise over time, and include other results in Appendix E.

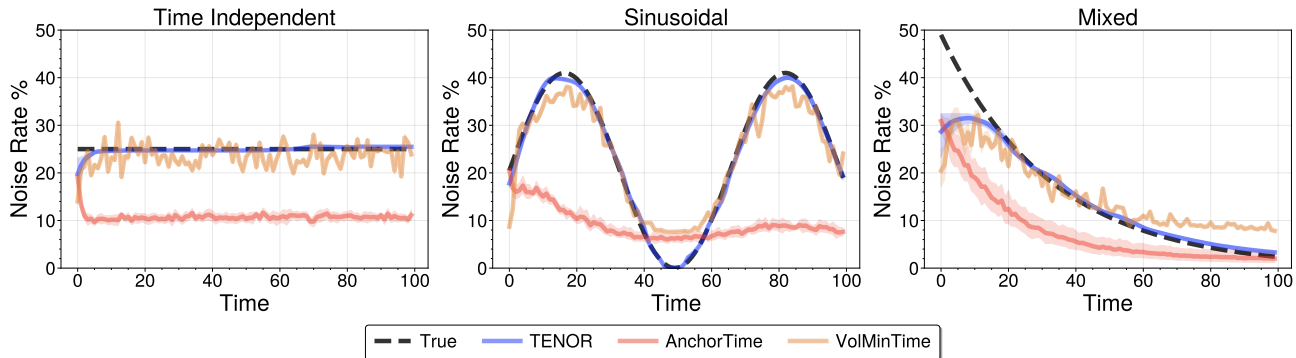


Figure 2: TENOR can learn temporal patterns in label noise across different noise patterns. The resulting noise model has lower reconstruction error than alternative approaches. We show results for *Mixed* noise, which denotes class-conditional noise where one class has increasing noise and one class has decreasing noise over time. We show the noise rate for the negative class only for clarity.

Table 2 shows the performance of each method on all five datasets. We find that overall, the temporal methods are consistently more accurate than their non-temporal counterparts highlighting the importance of modelling temporal noise in these settings. Among the temporal methods, TENOR achieves the best performance in comparison to AnchorTime and VolMinTime. TENOR’s superiority is even clearer when compared to the original non-temporal versions of these methods. Table 3 indicates that these benefits hold across different functional forms of label noise. More importantly, the benefit of TENOR becomes more evident as the amount of noise increases in the data (Fig. 3). In all these cases, we observe that the temporal methods are consistently more robust to both temporal and static label noise. Overall, these findings suggest that we can improve performance by explicitly modeling how noise varies across time instead of assuming it is distributed uniformly in time.

On Reconstructing the Temporal Noise Function We note that TENOR also achieves the best reconstruction error on all datasets in terms of MAE (Table 2). These results suggest that performance gains from our method are linked to how well we estimate the temporal label noise function. Qualitatively, we can compare our estimated noise functions

and the ground truth for TENOR and baselines in Fig. 2. We can see that our method consistently estimates the noise function with lower mean absolute error across different families of noise functions. Extended results on all other datasets (including multiclass) are present in Appendix E.

On the Risk of Misspecification We next demonstrate the limitations of *static* approaches, as they misspecify the noise function. As our theoretical results in Section 2.2 show, we expect that accurately specifying the noise process can lead to noise-tolerant models. However, existing Q -estimators assume label noise is static. We validate this experimentally by comparing our *forward sequence loss* method using the true temporal noise function vs. a static approximation (average of noise over time). As shown in Fig. 5 (Appendix E), the static (*mis*-)specification consistently leads to poor performance. These differences are more pronounced in the *Mixed* noise function, suggesting that class-conditional noise may exacerbate this weakness. The *forward sequence loss* shows consistent improvements when we correctly specify the temporal label noise function. In contrast, we observe inconsistent effects for the *backward sequence loss* technique. For example, correct specification leads to worse performance in the *Sinusoidal* noise setting,

Learning from Time Series under Temporal Label Noise

		Time Independent		Exponential		Linear		Sigmoidal		Sinusoidal		Mixed	
		Accuracy \uparrow	MAE \downarrow	Accuracy \uparrow	MAE \downarrow	Accuracy \uparrow	MAE \downarrow	Accuracy \uparrow	MAE \downarrow	Accuracy \uparrow	MAE \downarrow	Accuracy \uparrow	MAE \downarrow
Static	Uncorrected	75.5 \pm 2.2	–	70.0 \pm 3.2	–	72.9 \pm 3.3	–	74.0 \pm 2.3	–	76.0 \pm 5.1	–	70.6 \pm 3.0	–
	Anchor	86.2 \pm 2.7	.04 \pm .01	80.6 \pm 2.3	.08 \pm .01	78.1 \pm 2.4	.12 \pm .02	82.4 \pm 5.9	.16 \pm .01	82.0 \pm 3.6	.15 \pm .01	79.1 \pm 2.6	.13 \pm .01
	VolMinNet	88.3 \pm 2.1	.02 \pm .01	81.3 \pm 2.0	.07 \pm .01	81.9 \pm 3.4	.10 \pm .02	81.6 \pm 2.5	.14 \pm .00	86.5 \pm 6.0	.13 \pm .01	85.1 \pm 2.7	.11 \pm .00
Temporal	AnchorTime	86.1 \pm 4.5	.06 \pm .01	80.6 \pm 2.5	.08 \pm .01	78.0 \pm 2.2	.11 \pm .01	80.7 \pm 2.7	.14 \pm .01	81.5 \pm 4.3	.14 \pm .01	80.0 \pm 1.8	.11 \pm .01
	VolMinTime	86.7 \pm 1.6	.08 \pm .00	79.5 \pm 3.3	.11 \pm .01	81.8 \pm 4.2	.10 \pm .02	83.1 \pm 3.0	.12 \pm .01	85.3 \pm 5.7	.11 \pm .01	82.4 \pm 2.7	.10 \pm .00
	TENOR	97.9\pm0.7	.01\pm.00	96.6\pm1.1	.03\pm.01	94.9\pm4.4	.03\pm.02	98.2\pm0.5	.02\pm.01	98.3\pm0.6	.03\pm.01	95.8\pm2.2	.03\pm.01

Table 3: Clean test set accuracy (%) and reconstruction error MAE ($\hat{Q}(t)$) for all methods and temporal label noise functions with 30% label noise on average. We report the mean value \pm st.dev for each metric over 10 runs, and highlight the methods that achieve the best results in **green**. We show results for `har` dataset and include complete results in Appendix E.

but better performance for *Mixed* noise. We discuss potential reasons for this inconsistency in Appendix E.

On Choosing between Loss Correction Techniques Our results highlight an important consideration in choosing between the *forward sequence loss* and *backward sequence loss* loss in sequential classification tasks. Although these losses have similar robustness guarantees, Fig. 5 (Appendix E) shows that the *forward sequence loss* technique consistently outperforms the *backward sequence loss* technique across all types and amounts of label noise. These results hold in experiments where we know the noise function $Q(t)$ – that is, even if we could *perfectly* estimate the noise process, the *backward sequence loss* underperforms. These results reflect a key issue in optimizing the *backward sequence loss* in sequential classification tasks, as the procedure requires repeated scaling of the loss function with an inverse matrix at each time step. This can lead to numerical instability in gradient backpropagation. This is the *best case* scenario where the noise function is perfectly specified, indicating irreducible limitations of the *backward sequence loss*. A detailed analysis is provided in Appendix E.

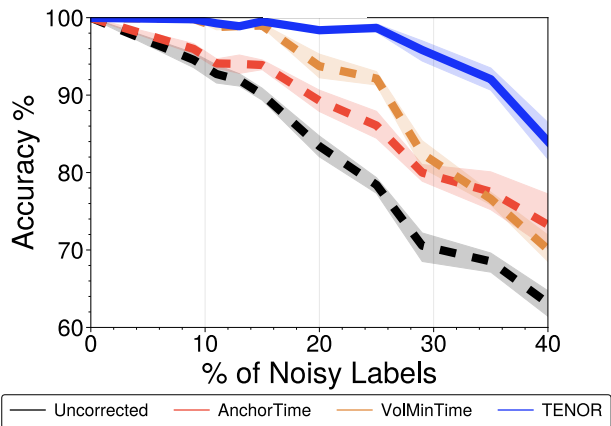


Figure 3: TENOR has consistently higher clean test set accuracy (%) than other temporal methods across *all* levels of noise. We show results for `har` and *Mixed* label noise shown. Error bars are st. dev. over 10 runs.

5. Concluding Remarks

Many classification tasks, such as those found in healthcare, require classifying labels in a sequential fashion under unobserved label noise. It is well-known that noisy labels cause problems for static classification. In time series, however, labels that are observed sequentially may admit differing noise rates over time. For example, label quality may improve or worsen over time. Existing methods work to construct noise-tolerant classifiers in the static setting and are ill-equipped to handle temporal label noise. Our work shows existing methods substantially underperform when subject to *temporal label noise*. To mitigate this, we show how to learn provably robust classifiers from sequential data that have been corrupted with temporal label noise using knowledge of the underlying noise function. Given that the noise function is often unknown, we also propose methods to learn noise-tolerant time series classifiers without prior knowledge of the temporal noise function.

Limitations Our methods rely on Assumption 1 and 2. Though these are standard assumptions in sequential modeling, they may be difficult to verify in practice. Additionally, though we provide equivalence statements in Theorem 2 and Theorem 1, finite-sample guarantees may be more indicative of performance. Using the equivalences we derive, finite-sample guarantees and excess-risk bounds may be drawn from existing results.

Lastly, we assume that all sequences in a dataset have the same underlying label noise function. This may not be true as different annotators can introduce differing noise patterns. We can potentially relax this assumption by considering multi-annotator noisy labels works [56, 31, 63] or generative models that admit clusters of temporal noise patterns (*i.e.*, mixture modeling). Lastly, we intentionally leave our Def. 1 generalizable to continuous time models. We represented the estimated temporal label noise function as a feed-forward neural network. In general, however, this can be parameterized however a user sees fit—*e.g.*, a time-dependent noise function could be obtained using a Gaussian Process or a neural ODE.

Impact Statement

This paper aims to advance the field of machine learning by highlighting an important issue in time-series modelling. Our approach is designed to capture label noise that evolves over time, under the assumption that this rate changes uniformly across individuals. However, in practice, it's plausible that noise rates vary among different groups [67]. This acknowledgment enriches the ongoing dialogue about label noise, fairness, and accuracy in machine learning algorithms.

References

- [1] Aroyo, L. and Welty, C. Truth is a lie: Crowd truth and the seven myths of human annotation. *AI Magazine*, 36(1): 15–24, 2015.
- [2] Arpit, D., Jastrzëbski, S., Ballas, N., Krueger, D., Bengio, E., Kanwal, M. S., Maharaj, T., Fischer, A., Courville, A., Bengio, Y., et al. A closer look at memorization in deep networks. In *International Conference on Machine Learning*, pp. 233–242. PMLR, 2017.
- [3] Atkinson, G. and Metsis, V. Identifying label noise in time-series datasets. In *Adjunct Proceedings of the 2020 ACM International Joint Conference on Pervasive and Ubiquitous Computing and Proceedings of the 2020 ACM International Symposium on Wearable Computers*, pp. 238–243, 2020.
- [4] Beigman, E. and Klebanov, B. B. Learning with annotation noise. In *Proceedings of the Joint Conference of the 47th Annual Meeting of the ACL and the 4th International Joint Conference on Natural Language Processing of the AFNLP*, pp. 280–287, 2009.
- [5] Bengio, Y., Ducharme, R., and Vincent, P. A neural probabilistic language model. *Advances in Neural Information Processing Systems*, 13, 2000.
- [6] Bertrand, M. and Mullainathan, S. Do people mean what they say? implications for subjective survey data. *American Economic Review*, 91(2):67–72, 2001.
- [7] Bertsekas, D. P. *Constrained optimization and Lagrange multiplier methods*. Academic press, 2014.
- [8] Carpenter, C. Seasonal variation in self-reports of recent alcohol consumption: racial and ethnic differences. *Journal of Studies on Alcohol*, 64(3):415–418, 2003.
- [9] Cho, K., Van Merriënboer, B., Gulcehre, C., Bahdanau, D., Bougares, F., Schwenk, H., and Bengio, Y. Learning phrase representations using rnn encoder-decoder for statistical machine translation. *arXiv preprint arXiv:1406.1078*, 2014.
- [10] Choe, Y. J., Shin, J., and Spencer, N. Probabilistic interpretations of recurrent neural networks. *Probabilistic Graphical Models*, 2017.
- [11] Choi, E., Schuetz, A., Stewart, W. F., and Sun, J. Using recurrent neural network models for early detection of heart failure onset. *Journal of the American Medical Informatics Association*, 24(2):361–370, 2017.
- [12] Cui, B., Zhang, M., Xu, M., Wang, A., Yuan, W., and Ren, H. Rectifying noisy labels with sequential prior: Multi-scale temporal feature affinity learning for robust video segmentation. *arXiv preprint arXiv:2307.05898*, 2023.
- [13] Day, T. G., Simpson, J. M., Razavi, R., and Kainz, B. Improving image labelling quality. *Nature Machine Intelligence*, 5(4):335–336, 2023.
- [14] Duan, H., Sun, Z., Dong, W., He, K., and Huang, Z. On clinical event prediction in patient treatment trajectory using longitudinal electronic health records. *IEEE Journal of Biomedical and Health Informatics*, 24(7):2053–2063, 2019.
- [15] Feldman, V. Does learning require memorization? a short tale about a long tail. In *Proceedings of the 52nd Annual ACM SIGACT Symposium on Theory of Computing*, pp. 954–959, 2020.
- [16] Feldman, V. and Zhang, C. What neural networks memorize and why: Discovering the long tail via influence estimation. *Advances in Neural Information Processing Systems*, 33: 2881–2891, 2020.
- [17] Folkard, S. Diurnal variation in logical reasoning. *British Journal of Psychology*, 66(1):1–8, 1975.
- [18] Frénay, B. and Verleysen, M. Classification in the presence of label noise: a survey. *IEEE Transactions on Neural Networks and Learning Systems*, 25(5):845–869, 2013.
- [19] Gandhi, T. K. and Singh, H. Reducing the risk of diagnostic error in the covid-19 era. *Journal of Hospital Medicine*, 15(6):363, 2020.
- [20] Ghosh, A., Kumar, H., and Sastry, P. S. Robust loss functions under label noise for deep neural networks. In *Proceedings of the AAAI Conference on Artificial Intelligence*, volume 31, 2017.
- [21] Goldberger, A. L., Amaral, L. A., Glass, L., Hausdorff, J. M., Ivanov, P. C., Mark, R. G., Mietus, J. E., Moody, G. B., Peng, C.-K., and Stanley, H. E. Physiobank, physiotoolkit, and physionet: components of a new research resource for complex physiologic signals. *Circulation*, 101(23):e215–e220, 2000.
- [22] Han, B., Yao, Q., Yu, X., Niu, G., Xu, M., Hu, W., Tsang, I., and Sugiyama, M. Co-teaching: Robust training of deep neural networks with extremely noisy labels. *Advances in Neural Information Processing Systems*, 31, 2018.
- [23] Han, B., Yao, Q., Liu, T., Niu, G., Tsang, I. W., Kwok, J. T., and Sugiyama, M. A survey of label-noise representation learning: Past, present and future. *arXiv preprint arXiv:2011.04406*, 2020.
- [24] Harutyunyan, H., Reing, K., Ver Steeg, G., and Galstyan, A. Improving generalization by controlling label-noise information in neural network weights. In *International Conference on Machine Learning*, pp. 4071–4081. PMLR, 2020.
- [25] Hsieh, G. and Kocielnik, R. You get who you pay for: The impact of incentives on participation bias. In *Proceedings of the 19th ACM Conference on Computer-supported Cooperative work & Social Computing*, pp. 823–835, 2016.

- [26] Inel, O., Khamkham, K., Cristea, T., Dumitrache, A., Rutjes, A., van der Ploeg, J., Romaszko, L., Aroyo, L., and Sips, R.-J. Crowdttruth: Machine-human computation framework for harnessing disagreement in gathering annotated data. In *The Semantic Web—ISWC 2014: 13th International Semantic Web Conference, Riva del Garda, Italy, October 19-23, 2014. Proceedings, Part II 13*, pp. 486–504. Springer, 2014.
- [27] Jambigi, N., Chanda, T., Unnikrishnan, V., and Spiliopoulou, M. Assessing the difficulty of labelling an instance in crowdworking. In *Workshops of the European Conference on Machine Learning and Knowledge Discovery in Databases*, pp. 363–373. Springer, 2020.
- [28] Jung, H., Park, Y., and Lease, M. Predicting next label quality: A time-series model of crowdwork. In *Proceedings of the AAAI Conference on Human Computation and Crowdsourcing*, volume 2, pp. 87–95, 2014.
- [29] Kiyokawa, T., Tomochika, K., Takamatsu, J., and Ogasawara, T. Fully automated annotation with noise-masked visual markers for deep-learning-based object detection. *IEEE Robotics and Automation Letters*, 4(2):1972–1977, 2019.
- [30] Lee, J. M. and Hauskrecht, M. Modeling multivariate clinical event time-series with recurrent temporal mechanisms. *Artificial intelligence in medicine*, 112:102021, 2021.
- [31] Li, S., Ge, S., Hua, Y., Zhang, C., Wen, H., Liu, T., and Wang, W. Coupled-view deep classifier learning from multiple noisy annotators. In *Proceedings of the AAAI Conference on Artificial Intelligence*, volume 34, pp. 4667–4674, 2020.
- [32] Li, S., Xia, X., Zhang, H., Zhan, Y., Ge, S., and Liu, T. Estimating noise transition matrix with label correlations for noisy multi-label learning. *Advances in Neural Information Processing Systems*, 35:24184–24198, 2022.
- [33] Li, X., Liu, T., Han, B., Niu, G., and Sugiyama, M. Provably end-to-end label-noise learning without anchor points. In *International Conference on Machine Learning*, pp. 6403–6413. PMLR, 2021.
- [34] Lipton, Z. C., Kale, D. C., Elkan, C., and Wetzel, R. Learning to diagnose with lstm recurrent neural networks. *arXiv preprint arXiv:1511.03677*, 2015.
- [35] Lipton, Z. C., Kale, D., and Wetzel, R. Directly modeling missing data in sequences with rnns: Improved classification of clinical time series. In *Machine learning for healthcare conference*, pp. 253–270. PMLR, 2016.
- [36] Liu, S., Niles-Weed, J., Razavian, N., and Fernandez-Granda, C. Early-learning regularization prevents memorization of noisy labels. *Advances in Neural Information Processing Systems*, 33:20331–20342, 2020.
- [37] Liu, T. and Tao, D. Classification with noisy labels by importance reweighting. *IEEE Transactions on Pattern Analysis and Machine Intelligence*, 38(3):447–461, 2015.
- [38] Liu, Y. and Guo, H. Peer loss functions: Learning from noisy labels without knowing noise rates. In *International Conference on Machine Learning*, pp. 6226–6236. PMLR, 2020.
- [39] Logacjov, A. and Ustad, A. HAR70+. UCI Machine Learning Repository, 2023. DOI: <https://doi.org/10.24432/C5CW3D>.
- [40] Long, P. M. and Servedio, R. A. Random classification noise defeats all convex potential boosters. In *International Conference on Machine Learning*, pp. 608–615, 2008.
- [41] Natarajan, N., Dhillon, I. S., Ravikumar, P. K., and Tewari, A. Learning with noisy labels. *Advances in Neural Information Processing Systems*, 26, 2013.
- [42] Norden, M., Wolf, O. T., Lehmann, L., Langer, K., Lippert, C., and Drimalla, H. Automatic detection of subjective, annotated and physiological stress responses from video data. In *10th International Conference on Affective Computing and Intelligent Interaction (ACII)*, pp. 1–8. IEEE, 2022.
- [43] Patrini, G., Rozza, A., Krishna Menon, A., Nock, R., and Qu, L. Making deep neural networks robust to label noise: A loss correction approach. In *Proceedings of the IEEE Conference on Computer Vision and Pattern Recognition*, pp. 1944–1952, 2017.
- [44] Peacock, H. M., De Gendt, C., Silversmit, G., Nuyts, S., Casselman, J., Machiels, J.-P., Giusti, F., Van Gool, B., Van der Poorten, V., and Van Eycken, L. Stage shift and relative survival for head and neck cancer during the 2020 covid-19 pandemic: a population-based study of temporal trends. *Frontiers in Oncology*, 13, 2023.
- [45] Phan, H., Andreotti, F., Cooray, N., Chén, O. Y., and De Vos, M. Seqsleepnet: end-to-end hierarchical recurrent neural network for sequence-to-sequence automatic sleep staging. *IEEE Transactions on Neural Systems and Rehabilitation Engineering*, 27(3):400–410, 2019.
- [46] Philbrick, K. A., Weston, A. D., Akkus, Z., Kline, T. L., Korfiatis, P., Sakinis, T., Kostandy, P., Boonrod, A., Zeinoddini, A., Takahashi, N., et al. Ril-contour: a medical imaging dataset annotation tool for and with deep learning. *Journal of Digital Imaging*, 32:571–581, 2019.
- [47] Pierson, E., Althoff, T., Thomas, D., Hillard, P., and Leskovec, J. Daily, weekly, seasonal and menstrual cycles in women’s mood, behaviour and vital signs. *Nature Human Behaviour*, 5(6):716–725, 2021.
- [48] Pusic, M. V., Rapkiewicz, A., Raykov, T., and Melamed, J. Estimating the irreducible uncertainty in visual diagnosis: Statistical modeling of skill using response models. *Medical Decision Making*, 43(6):680–691, 2023.
- [49] Quisel, T., Foschini, L., Signorini, A., and Kale, D. C. Collecting and analyzing millions of mhealth data streams. In *Proceedings of the 23rd ACM SIGKDD International Conference on Knowledge Discovery and Data Mining*, pp. 1971–1980, 2017.
- [50] Raykar, V. C., Yu, S., Zhao, L. H., Valadez, G. H., Florin, C., Bogoni, L., and Moy, L. Learning from crowds. *Journal of Machine Learning Research*, 11(4), 2010.
- [51] Reid, M. D. and Williamson, R. C. Composite binary losses. *Journal of Machine Learning Research*, 11(83):2387–2422, 2010. URL <http://jmlr.org/papers/v11/reid10a.html>.
- [52] Reyes-Ortiz, J., Anguita, D., Ghio, A., Oneto, L., and Parra, X. Human Activity Recognition Using Smartphones. UCI Machine Learning Repository, 2012. DOI: <https://doi.org/10.24432/C54S4K>.

- [53] Roesler, O. EEG Eye State. UCI Machine Learning Repository, 2013. DOI: <https://doi.org/10.24432/C57G7J>.
- [54] Sano, A. and Picard, R. W. Stress recognition using wearable sensors and mobile phones. In *2013 Humaine Association Conference on Affective Computing and Intelligent Interaction*, pp. 671–676. IEEE, 2013.
- [55] Schaekermann, M., Law, E., Larson, K., and Lim, A. Expert disagreement in sequential labeling: A case study on adjudication in medical time series analysis. In *SAD/CrowdBias@HCOMP*, pp. 55–66, 2018.
- [56] Schmarje, L., Grossmann, V., Zelenka, C., Dippel, S., Kiko, R., Oszust, M., Pastell, M., Stracke, J., Valros, A., Volkmann, N., et al. Is one annotation enough?-a data-centric image classification benchmark for noisy and ambiguous label estimation. *Advances in Neural Information Processing Systems*, 35:33215–33232, 2022.
- [57] Sha, Y. and Wang, M. D. Interpretable predictions of clinical outcomes with an attention-based recurrent neural network. In *Proceedings of the 8th ACM International Conference on Bioinformatics, Computational Biology, and Health Informatics*, pp. 233–240, 2017.
- [58] Shamshirband, S., Fathi, M., Dehzangi, A., Chronopoulos, A. T., and Alinejad-Rokny, H. A review on deep learning approaches in healthcare systems: Taxonomies, challenges, and open issues. *Journal of Biomedical Informatics*, 113:103627, 2021.
- [59] Shekelle, P., Eccles, M. P., Grimshaw, J. M., and Woolf, S. H. When should clinical guidelines be updated? *Bmj*, 323(7305):155–157, 2001.
- [60] Sugiyama, M., Liu, T., Han, B., Liu, Y., and Niu, G. Learning and mining with noisy labels. In *Proceedings of the 31st ACM International Conference on Information & Knowledge Management*, pp. 5152–5155, 2022.
- [61] Suo, Q., Ma, F., Canino, G., Gao, J., Zhang, A., Veltri, P., and Agostino, G. A multi-task framework for monitoring health conditions via attention-based recurrent neural networks. In *AMIA annual symposium proceedings*, volume 2017, pp. 1665. American Medical Informatics Association, 2017.
- [62] Sutskever, I., Vinyals, O., and Le, Q. V. Sequence to sequence learning with neural networks. *Advances in neural information processing systems*, 27, 2014.
- [63] Tanno, R., Saeedi, A., Sankaranarayanan, S., Alexander, D. C., and Silberman, N. Learning from noisy labels by regularized estimation of annotator confusion. In *Proceedings of the IEEE/CVF conference on computer vision and pattern recognition*, pp. 11244–11253, 2019.
- [64] Vaizman, Y., Ellis, K., and Lanckriet, G. Recognizing detailed human context in the wild from smartphones and smartwatches. *IEEE pervasive computing*, 16(4):62–74, 2017.
- [65] Vaswani, A., Shazeer, N., Parmar, N., Uszkoreit, J., Jones, L., Gomez, A. N., Kaiser, Ł., and Polosukhin, I. Attention is all you need. *Advances in neural information processing systems*, 30, 2017.
- [66] Wallace, S., Cai, T., Le, B., and Leiva, L. A. Debiased label aggregation for subjective crowdsourcing tasks. In *CHI Conference on Human Factors in Computing Systems Extended Abstracts*, pp. 1–8, 2022.
- [67] Wang, J., Liu, Y., and Levy, C. Fair classification with group-dependent label noise. In *Proceedings of the 2021 ACM Conference on Fairness, Accountability, and Transparency*, FAccT ’21, pp. 526–536, New York, NY, USA, 2021. Association for Computing Machinery. ISBN 9781450383097. doi: 10.1145/3442188.3445915. URL <https://doi.org/10.1145/3442188.3445915>.
- [68] Wang, L., Zhang, W., He, X., and Zha, H. Supervised reinforcement learning with recurrent neural network for dynamic treatment recommendation. In *Proceedings of the 24th ACM SIGKDD international conference on knowledge discovery & data mining*, pp. 2447–2456, 2018.
- [69] Wang, Y., Ma, X., Chen, Z., Luo, Y., Yi, J., and Bailey, J. Symmetric cross entropy for robust learning with noisy labels. In *Proceedings of the IEEE/CVF International Conference on Computer Vision*, pp. 322–330, 2019.
- [70] Wei, J., Zhu, Z., Cheng, H., Liu, T., Niu, G., and Liu, Y. Learning with noisy labels revisited: A study using real-world human annotations. *arXiv preprint arXiv:2110.12088*, 2021.
- [71] Westbrook, J. I., Coiera, E., Dunsmuir, W. T., Brown, B. M., Kelk, N., Paoloni, R., and Tran, C. The impact of interruptions on clinical task completion. *BMJ Quality & Safety*, 19(4):284–289, 2010.
- [72] Whitehill, J., Wu, T.-f., Bergsma, J., Movellan, J., and Ruvolo, P. Whose vote should count more: Optimal integration of labels from labelers of unknown expertise. *Advances in Neural Information Processing Systems*, 22, 2009.
- [73] Xia, X., Liu, T., Wang, N., Han, B., Gong, C., Niu, G., and Sugiyama, M. Are anchor points really indispensable in label-noise learning? *Advances in Neural Information Processing Systems*, 32, 2019.
- [74] Xiao, T., Xia, T., Yang, Y., Huang, C., and Wang, X. Learning from massive noisy labeled data for image classification. In *Proceedings of the IEEE conference on Computer Vision and Pattern Recognition*, pp. 2691–2699, 2015.
- [75] Yao, Y., Liu, T., Han, B., Gong, M., Deng, J., Niu, G., and Sugiyama, M. Dual t: Reducing estimation error for transition matrix in label-noise learning. *Advances in Neural Information Processing Systems*, 33:7260–7271, 2020.
- [76] Yong, L., Pi, R., Zhang, W., Xia, X., Gao, J., Zhou, X., Liu, T., and Han, B. A holistic view of label noise transition matrix in deep learning and beyond. In *International Conference on Learning Representations*, 2023.
- [77] Yu, X., Han, B., Yao, J., Niu, G., Tsang, I., and Sugiyama, M. How does disagreement help generalization against label corruption? In *International Conference on Machine Learning*, pp. 7164–7173. PMLR, 2019.
- [78] Zhang, S., Yu, J., Xu, X., Yin, C., Lu, Y., Yao, B., Tory, M., Padilla, L. M., Caterino, J., Zhang, P., et al. Rethinking human-ai collaboration in complex medical decision making: A case study in sepsis diagnosis. *arXiv preprint arXiv:2309.12368*, 2023.

- [79] Zhang, Y., Niu, G., and Sugiyama, M. Learning noise transition matrix from only noisy labels via total variation regularization. In *International Conference on Machine Learning*, pp. 12501–12512. PMLR, 2021.

A. Proofs

In what follows, we use vector notation for completeness and clarity of exposition.

We make the following assumptions regarding the conditional time series distribution for the clean labels $p(\mathbf{y}_{1:T} \mid \mathbf{x}_{1:T})$ and noisy labels $p(\tilde{\mathbf{y}}_{1:T} \mid \mathbf{x}_{1:T})$:

We make the following assumptions about the clean data distribution:

Assumption 3. *The clean labels y_t at times $t = 1, \dots, T$ are conditionally independent given the features observed up to time t $\mathbf{x}_{1:t}$.*

$$y_t \perp\!\!\!\perp y_{1:t-1} \mid \mathbf{x}_{1:t} \quad (7)$$

Assumption 4. *The clean labels y_t at time t is conditionally independent from \mathbf{x}_{t+1} given $\mathbf{x}_{1:t}$:*

$$p(\mathbf{y}_{1:T} \mid \mathbf{x}_{1:T}) = \prod_{t=1}^T p(y_t \mid \mathbf{x}_{1:t}). \quad (8)$$

Assumption 5. *The noisy labels at time t \tilde{y}_t are conditionally independent of $\mathbf{x}_{1:t}$ given the clean labels y_t at time t .*

$$p(\tilde{y}_t \mid \mathbf{x}_{1:t}) = \sum_{c=1}^C q_t(\tilde{y}_t \mid y_t = c) p(y_t = c \mid \mathbf{x}_{1:t}) \quad (9)$$

Note that the following property follows from the above assumptions:

$$p(\tilde{\mathbf{y}}_{1:T} \mid \mathbf{x}_{1:T}) = \prod_{t=1}^T q_t(\tilde{y}_t \mid \mathbf{x}_{1:t}). \quad (10)$$

Definitions We start by defining some of the quantities that will be important for our forward and backward proofs:

$p(y_t \mid \mathbf{x}_{1:t}) := [p(y_t = c \mid \mathbf{x}_{1:t})]_{c=1:C}^\top \in \mathbb{R}^{C \times 1}$ (Vector of probabilities for each label value, for the clean label distribution)

$p(\tilde{y}_t \mid \mathbf{x}_{1:t}) := [p(y_t = c \mid \mathbf{x}_{1:t})]_{c=1:C}^\top \in \mathbb{R}^{C \times 1}$ (Vector of probabilities for each possible label value, for the noisy label distribution)

$\mathbf{h}_\theta(\mathbf{x}_{1:t}) = \mathbf{p}_\theta(y_t \mid \mathbf{x}_{1:t} = \mathbf{x}_{1:t}) : \mathbb{R}^{d \times t} \rightarrow \mathbb{R}^C$ (Classifier that predicts label distribution at t given preceding observations)

$\mathbf{h}_\theta(\mathbf{x}_{1:t}) = \psi^{-1}(g_\theta(\mathbf{x}_{1:t}))$ (When h_θ is a deep network, g_θ is the final logits and $\psi : \Delta^{C-1} \rightarrow \mathbb{R}^C$ represents an invertible link function whose inverse maps the logits to a valid probability; i.e. a softmax function). We thus assume that

$\mathbf{Q}_t := [q_t(\tilde{y}_t = k \mid y_t = j)]_{j,k} \in \mathbb{R}^{C \times C}$ (The temporal noise matrix at time t)

$\ell_t(y_t, \mathbf{h}_\theta(\mathbf{x}_{1:t})) = -\log p_\theta(y_t = y_t \mid \mathbf{x}_{1:t} = \mathbf{x}_{1:t}) : \mathcal{Y} \times \mathbb{R}^C \rightarrow \mathbb{R}$ (loss at t)

$\ell_{\psi,t}(y_t, \mathbf{h}_\theta(\mathbf{x}_{1:t})) = \ell_t(y_t, \psi^{-1} \mathbf{h}_\theta(\mathbf{x}_{1:t}))$ (A composite loss function is a loss function that uses the aid of a link function: ψ)

$\ell_t(\mathbf{h}_\theta(\mathbf{x}_{1:t})) = [\ell_t(c, \mathbf{h}_\theta(\mathbf{x}_{1:t}))]_{c=1:C}^\top : \mathbb{R}^C \rightarrow \mathbb{R}^C$ (vector of NLL losses, for each possible value of the ground truth)

$\overleftarrow{\ell}_t(\mathbf{h}_\theta(\mathbf{x}_{1:t})) = \mathbf{Q}_t^{-1} \ell_t(\mathbf{h}_\theta(\mathbf{x}_{1:t})) = [\overleftarrow{\ell}_t(c, \mathbf{h}_\theta(\mathbf{x}_{1:t}))]_{c=1:C}^\top : \mathbb{R}^C \rightarrow \mathbb{R}^C$ (vector of $\overleftarrow{\ell}_t(\cdot, \cdot)$ losses, for each possible value of the ground truth)

$$\overleftarrow{\ell}_t(c, \mathbf{h}_\theta(\mathbf{x}_{1:t})) = [\mathbf{Q}_t^{-1}]_{c,:} \cdot \ell(\mathbf{h}_\theta(\mathbf{x}_{1:t}))$$

$$\overrightarrow{\ell}_{t,\psi}(c, \mathbf{h}_\theta(\mathbf{x}_{1:t})) = \ell_t(c, \mathbf{Q}_t^\top \cdot \psi^{-1}(\mathbf{g}_\theta))$$

$$\overrightarrow{\ell}_{seq,\psi}(\mathbf{y}_{1:T}, \mathbf{h}_\theta(\mathbf{x}_{1:t})) = \sum_{t=1}^\top \overrightarrow{\ell}_{t,\psi}(c, \mathbf{h}_\theta(\mathbf{x}_{1:t}))$$

Lemma 1. $\mathbb{E}_{\mathbf{y}_{1:T}|\mathbf{x}_{1:T}} \log p(y_t | \mathbf{x}_{1:T}) = \mathbb{E}_{\mathbf{y}_t|\mathbf{x}_{1:t}} \log p(y_t | \mathbf{x}_{1:t})$

Proof.

$$\begin{aligned} \mathbb{E}_{\mathbf{y}_{1:T}|\mathbf{x}_{1:T}} \log(p(y_t | \mathbf{x}_{1:T})) &= \sum_{c_1} \sum_{c_2} \dots \sum_{c_T} p(y_1 = c_1, y_2 = c_2, \dots, y_T = c_T | \mathbf{x}_{1:T}) \\ &\quad \log(p(y_t = c_t | \mathbf{x}_{1:T})) \\ &= \sum_c \sum_{c_1} \dots \sum_{c_T} p(y_1 = c_1, y_2 = c_2, \dots, y_{t-1} = c_{t-1} | \mathbf{x}_{1:T}) \\ &\quad * p(y_{t+1} = c_{t+1}, \dots, y_T = c_T | \mathbf{x}_{1:T}) * p(y_t = c_t | \mathbf{x}_{1:T}) \\ &\quad * \log(p(y_t = c_t | \mathbf{x}_{1:T})) \\ &= \sum_{c_1} \sum_{c_2} \dots \sum_{c_T} p(y_1 = c_1, y_2 = c_2, \dots, y_{t-1} = c_{t-1} | \mathbf{x}_{1:t-1}) \\ &\quad * p(y_{t+1} = c_{t+1}, \dots, y_T = c_T | \mathbf{x}_{t+1:T}) * p(y_t = c_t | \mathbf{x}_{1:t}) \\ &\quad * \log(p(y_t = c_t | \mathbf{x}_{1:t})) \\ &= \mathbb{E}_{\mathbf{y}_{1:t-1}|\mathbf{x}_{1:t-1}} \mathbb{E}_{\mathbf{y}_{t+1:T}|\mathbf{x}_{t+1:T}} p(y_t = c_t | \mathbf{x}_{1:t}) \log(p(y_t = c_t | \mathbf{x}_{1:t})) \\ &= \mathbb{E}_{\mathbf{y}_{1:t-1}|\mathbf{x}_{1:t-1}} \mathbb{E}_{\mathbf{y}_{t+1:T}|\mathbf{x}_{t+1:T}} [\mathbb{E}_{\mathbf{y}_t|\mathbf{x}_{1:t}} \log(p(y_t | \mathbf{x}_{1:t}))] \\ &\quad \text{(Note that } [\mathbb{E}_{p(y_t|\mathbf{x}_{1:T})} \log(p(y_t | \mathbf{x}_{1:t}))] \text{ is constant)} \\ &= \mathbb{E}_{p(y_t|\mathbf{x}_{1:t})} \log(p(y_t | \mathbf{x}_{1:t})) \\ &\quad \text{(From property that } \mathbb{E}[C] = C \text{ for constant } C) \end{aligned}$$

□

Lemma 2. $\operatorname{argmax}_\theta \mathbb{E}_{\mathbf{y}_{1:T}|\mathbf{x}_{1:T}} \log(p_\theta(\mathbf{y}_{1:T} | \mathbf{x}_{1:T})) = \operatorname{argmin}_\theta \sum_{t=1}^\top \mathbb{E}_{\tilde{\mathbf{y}}_t|\mathbf{x}_{1:t}} \overleftarrow{\ell}_t(\tilde{\mathbf{y}}_t, \mathbf{h}_\theta(\mathbf{x}_{1:t}))$

Proof.

$$\begin{aligned}
 & \operatorname{argmax}_{\theta} \mathbb{E}_{\mathbf{y}_{1:T} | \mathbf{x}_{1:T}} \log (\mathbf{p}_{\theta}(\mathbf{y}_{1:T} | \mathbf{x}_{1:T})) \\
 &= \operatorname{argmax}_{\theta} \mathbb{E}_{\mathbf{y}_{1:T} | \mathbf{x}_{1:T}} \log \left(\prod_{t=1}^{\top} \mathbf{p}_{\theta}(y_t | \mathbf{x}_{1:t}) \right) && \text{(by Assumption 3)} \\
 &= \operatorname{argmax}_{\theta} \mathbb{E}_{\mathbf{y}_{1:T} | \mathbf{x}_{1:T}} \sum_{t=1}^{\top} \log (\mathbf{p}_{\theta}(y_t | \mathbf{x}_{1:t})) \\
 &= \operatorname{argmax}_{\theta} \sum_{t=1}^{\top} \mathbb{E}_{\mathbf{y}_{1:T} | \mathbf{x}_{1:T}} \log (\mathbf{p}_{\theta}(y_t | \mathbf{x}_{1:t})) && \text{(due to linearity of } \mathbb{E} \text{)} \\
 &= \operatorname{argmax}_{\theta} \sum_{t=1}^{\top} \mathbb{E}_{\mathbf{y}_t | \mathbf{x}_{1:t}} \log (\mathbf{p}_{\theta}(y_t | \mathbf{x}_{1:t})) && \text{(by Lemma 1)} \\
 &= \operatorname{argmin}_{\theta} \sum_{t=1}^{\top} \mathbb{E}_{\mathbf{y}_t | \mathbf{x}_{1:t}} \ell_t(y_t, \mathbf{h}_{\theta}(\mathbf{x}_{1:t})) && \text{(by definition of } \ell_t \text{)} \\
 &= \operatorname{argmin}_{\theta} \sum_{t=1}^{\top} \mathbf{p}(y_t | \mathbf{x}_{1:t})^{\top} \ell_t(\mathbf{h}_{\theta}(\mathbf{x}_{1:t})) \\
 &= \operatorname{argmin}_{\theta} \sum_{t=1}^{\top} \mathbf{p}(\tilde{y}_t | \mathbf{x}_{1:t})^{\top} \mathbf{Q}_t^{-1} \ell_t(\mathbf{h}_{\theta}(\mathbf{x}_{1:t})) \\
 &= \operatorname{argmin}_{\theta} \sum_{t=1}^{\top} \mathbf{p}(\tilde{y}_t | \mathbf{x}_{1:t})^{\top} \overleftarrow{\ell}_t(\mathbf{h}_{\theta}(\mathbf{x}_{1:t})) \\
 &= \operatorname{argmin}_{\theta} \sum_{t=1}^{\top} \mathbb{E}_{\tilde{y}_t | \mathbf{x}_{1:t}} [\overleftarrow{\ell}_t(\tilde{y}_t, \mathbf{h}_{\theta}(\mathbf{x}_{1:t}))]
 \end{aligned}$$

□

Theorem 3. Let $\overleftarrow{\ell}_{seq}(\tilde{\mathbf{y}}_{1:T}, \mathbf{h}_{\theta}(\mathbf{x}_{1:T})) = \sum_{t=1}^{\top} \overleftarrow{\ell}_t(\tilde{y}_t, \mathbf{h}_{\theta}(\mathbf{x}_{1:t}))$. Then,

$$\operatorname{argmax}_{\theta} \mathbb{E}_{\mathbf{y}_{1:T} | \mathbf{x}_{1:T}} \log (\mathbf{p}_{\theta}(\mathbf{y}_{1:T} | \mathbf{x}_{1:T})) = \operatorname{argmin}_{\theta} \mathbb{E}_{\tilde{\mathbf{y}}_{1:T} | \mathbf{x}_{1:T}} \overleftarrow{\ell}_{seq}(\tilde{\mathbf{y}}_{1:T}, \mathbf{h}_{\theta}(\mathbf{x}_{1:T}))$$

Proof.

$$\begin{aligned}
 \operatorname{argmin}_{\theta} \mathbb{E}_{\tilde{\mathbf{y}}_{1:T} | \mathbf{x}_{1:T}} \overleftarrow{\ell}_t(\tilde{\mathbf{y}}_{1:T}, \mathbf{h}_{\theta}(\mathbf{x}_{1:T})) &= \operatorname{argmin}_{\theta} \mathbb{E}_{\tilde{\mathbf{y}}_{1:T} | \mathbf{x}_{1:T}} \sum_{t=1}^{\top} \overleftarrow{\ell}_t(\tilde{y}_t, \mathbf{h}_{\theta}(\mathbf{x}_{1:t})) \\
 &= \operatorname{argmin}_{\theta} \sum_{t=1}^{\top} \mathbb{E}_{\tilde{\mathbf{y}}_{1:T} | \mathbf{x}_{1:T}} \overleftarrow{\ell}_t(\tilde{y}_t, \mathbf{h}_{\theta}(\mathbf{x}_{1:t})) \\
 &= \operatorname{argmin}_{\theta} \sum_{t=1}^{\top} \mathbb{E}_{\tilde{y}_t | \mathbf{x}_{1:t}} \overleftarrow{\ell}_t(\tilde{y}_t, \mathbf{h}_{\theta}(\mathbf{x}_{1:t})) && \text{(by Lemma 1)} \\
 &= \operatorname{argmax}_{\theta} \mathbb{E}_{\mathbf{y}_{1:T} | \mathbf{x}_{1:T}} \log (\mathbf{p}_{\theta}(\mathbf{y}_{1:T} | \mathbf{x}_{1:T})) && \text{(by Lemma 2)}
 \end{aligned}$$

□

Theorem 4. $\operatorname{argmin}_{\theta} \mathbb{E}_{\tilde{\mathbf{y}}_{1:T}, \mathbf{x}_{1:T}} \overrightarrow{\ell}_{seq, \psi}(\mathbf{y}_{1:T}, \mathbf{g}_{\theta}(\mathbf{x}_{1:T})) = \operatorname{argmin}_{\theta} \sum_{t=1}^{\top} \mathbb{E}_{\mathbf{y}_{1:t}, \mathbf{x}_{1:t}} \ell_{t, \phi}(\mathbf{y}_{1:T}, \mathbf{g}_{\theta}(\mathbf{x}_{1:T}))$.

Proof. First, note that:

$$\vec{\ell}_{t,\psi}(y_t, \mathbf{h}_\theta(\mathbf{x}_{1:t})) = \ell_t(y_t, \mathbf{Q}_t^\top \psi^{-1}(\mathbf{g}_\theta(\mathbf{x}_{1:t}))) \quad (11)$$

$$= \ell_{\phi_t,t}(y_t, \mathbf{g}_\theta(\mathbf{x}_{1:t})), \quad (12)$$

where $\phi_t^{-1} = \psi^{-1} \circ \mathbf{Q}_t^\top$. Thus, $\phi_t : \Delta^{C-1} \rightarrow \mathbb{R}^C$ is invertible, and is thus a proper composite loss [51].

Thus, as shown in Patrini et al. [43]:

$$\operatorname{argmin}_\theta \mathbb{E}_{\tilde{y}_t, \mathbf{x}_{1:t}} \ell_{\phi_t,t}(y_t, \mathbf{g}_\theta(\mathbf{x}_{1:t})) = \operatorname{argmin}_\theta \mathbb{E}_{\tilde{y}_t | \mathbf{x}_{1:t}} \ell_{\phi_t,t}(y_t, \mathbf{g}_\theta(\mathbf{x}_{1:t})) \quad (13)$$

$$= \phi_t(\mathbf{p}(\tilde{y}_t | \mathbf{x}_{1:t})) \quad (\text{property of proper composite losses})$$

$$= \psi((\mathbf{Q}_t^{-1})^\top \mathbf{p}(\tilde{y}_t | \mathbf{x}_{1:t})) \quad (14)$$

$$= \psi(\mathbf{p}(y_t | \mathbf{x}_{1:t})) \quad (15)$$

The above holds for the minimizer at a single time step, not the sequence as a whole. To find the minimizer of the loss over the entire sequence:

$$\operatorname{argmin}_\theta \mathbb{E}_{\mathbf{x}_{1:T}, \tilde{\mathbf{y}}_{1:T}} \vec{\ell}_{seq,\psi}(\tilde{\mathbf{y}}_{1:T}, \mathbf{g}_\theta(\mathbf{x}_{1:T})) = \operatorname{argmin}_\theta \mathbb{E}_{\tilde{\mathbf{y}}_{1:T} | \mathbf{x}_{1:T}} \vec{\ell}_{seq,\psi}(\tilde{\mathbf{y}}_{1:T}, \mathbf{g}_\theta(\mathbf{x}_{1:T})) \quad (16)$$

$$= \operatorname{argmin}_\theta \mathbb{E}_{\tilde{\mathbf{y}}_{1:T} | \mathbf{x}_{1:T}} \sum_{t=1}^T \vec{\ell}_{t,\psi}(\tilde{y}_t, \mathbf{g}_\theta(\mathbf{x}_{1:t})) \quad (17)$$

$$= \operatorname{argmin}_\theta \sum_{t=1}^T \mathbb{E}_{\tilde{y}_t | \mathbf{x}_{1:T}} \vec{\ell}_{t,\psi}(\tilde{y}_t, \mathbf{g}_\theta(\mathbf{x}_{1:t})) \quad (18)$$

$$= \operatorname{argmin}_\theta \sum_{t=1}^T \mathbb{E}_{\tilde{y}_t | \mathbf{x}_{1:t}} \vec{\ell}_{t,\psi}(\tilde{y}_t, \mathbf{g}_\theta(\mathbf{x}_{1:t})) \quad (19)$$

$$= \operatorname{argmin}_\theta \sum_{t=1}^T \mathbb{E}_{\tilde{y}_t | \mathbf{x}_{1:t}} \ell_{t,\phi}(\tilde{y}_t, \mathbf{g}_\theta(\mathbf{x}_{1:t})) \quad (20)$$

As the minimizer of the sum will be the function that minimizes each element of the sum, then $\operatorname{argmin}_\theta \mathbb{E}_{\tilde{\mathbf{y}}_{1:T}, \mathbf{x}_{1:T}} \vec{\ell}_{seq,\psi}(\mathbf{y}_{1:T}, \mathbf{g}_\theta(\mathbf{x}_{1:T})) = \psi(\mathbf{p}(\mathbf{y}_{1:T} | \mathbf{x}_{1:T}))$. Note that the $\operatorname{argmin}_\theta \sum_{t=1}^T \mathbb{E}_{\mathbf{y}_{1:t}, \mathbf{x}_{1:t}} \ell_{t,\phi}(\mathbf{y}_{1:t}, \mathbf{g}_\theta(\mathbf{x}_{1:t})) = \psi(\mathbf{p}(\mathbf{y}_{1:T} | \mathbf{x}_{1:T}))$, because the minimizer of the NLL is the data distribution. Thus, $\operatorname{argmin}_\theta \mathbb{E}_{\tilde{\mathbf{y}}_{1:T}, \mathbf{x}_{1:T}} \vec{\ell}_{seq,\psi}(\mathbf{y}_{1:T}, \mathbf{g}_\theta(\mathbf{x}_{1:T})) = \operatorname{argmin}_\theta \sum_{t=1}^T \mathbb{E}_{\mathbf{y}_{1:t}, \mathbf{x}_{1:t}} \ell_{t,\phi}(\mathbf{y}_{1:t}, \mathbf{g}_\theta(\mathbf{x}_{1:t}))$. \square

B. AnchorTime Procedure

1. Fit a probabilistic classifier to predict noisy labels from the observed data.
2. For each class $y \in \mathcal{Y}$ and time $t \in [1 \dots T]$:
 - i Identify anchor points for class y : $\tilde{\mathbf{x}}_t^j = \arg \max_{\mathbf{x}_t} p(\tilde{y}_t = y | \mathbf{x}_{1:t})$.
 - ii Set $\hat{Q}(t)_{y,y'}$ as the probability of classifier predicting class y' at time t given $\tilde{\mathbf{x}}_t^j$.

C. TENOR Learning Algorithm

We summarize the augmented Lagrangian approach to solving the TENOR objective in Algorithm 1

Algorithm 1 TENOR Learning Algorithm

Input: Noisy Training Dataset D , hyperparameters γ and η
Output: Model θ , Temporal Noise Function ω

```

 $c \leftarrow 1$  and  $\lambda \leftarrow 1$ 
for  $k = 1, 2, 3, \dots$  do
   $\theta^k, \omega^k = \arg \min_{\theta, \omega} \mathcal{L}(\theta, \omega)$  {Computed with SGD using the Adam optimizer}
   $\lambda \leftarrow \lambda + c * R_t(\theta^k, \omega^k)$  {Update Lagrange multiplier}
  if  $k > 0$  and  $R_t(\theta^k, \omega^k) > \gamma R_t(\theta^{k-1}, \omega^{k-1})$  then
     $c \leftarrow \eta c$ 
  else
     $c \leftarrow c$ 
  end if
  if  $R_t(\theta^k, \omega^k) == 0$  then
    break
  end if
end for

```

For all experiments we set $\lambda = 1, c = 1, \gamma = 2$, and $\eta = 2$. k and the maximum number of SGD iterations are set to 15 and 10, respectively. This is to ensure that the total number of epochs is 150, which is the max number of epochs used for all experiments.

D. Experimental Details

Dataset	Classification Task	n	d	T
eeg_eye [53]	Eye Open vs Eye Closed	299	14	50
eeg_sleep [21]	Sleep vs Awake	964	7	100
har [52]	Walking vs Not Walking	192	9	50
har70 [39]	Walking vs Not Walking	444	6	100
synth	[describe model in notation]	1,000	50	100

Table 4: Datasets used in the experiments. Classification tasks, number of samples (n), dimensionality at each time step (d), and sequence length (T) are shown.

D.1. Dataset Details

Synthetic We generate data for binary and multiclass classification with $n = 1\,000$ samples and $d = 50$ features over $T = 100$ time steps. We generate the class labels and observations for each time step using a Hidden Markov Model (HMM). The transition matrix generating the markov chain is uniform ensuring an equal likelihood of any state at any given time. We corrupted them using multidimensional (50) Gaussian emissions. The mean of the gaussian for state/class c is set to c with variance 1.5 (i.e. class 1 has mean 1 and variance 1.5). The high-dimensionality and overlap in feature-space between classes makes this a sufficiently difficult task, especially under label noise. We use a batchsize of 256

HAR from UC Irvine [52] consists of inertial sensor readings of 30 adult subjects performing activities of daily living. The sensor signals are already preprocessed and a vector of features at each time step are provided. We apply z-score normalization at the participant-level, then split the dataset into subsequences of a fixed size 50. We use a batchsize of 64.

HAR70 from UC Irvine [39] consists of inertial sensor readings of 18 elderly subjects performing activities of daily living. The sensor signals are already preprocessed and a vector of features at each time step are provided. We apply z-score normalization at the participant-level, then split the dataset into subsequences of a fixed size 100. We use a batchsize of 256.

EEG SLEEP from Physionet [21] consists of EEG data measured from 197 different whole nights of sleep observation, including awake periods at the start, end, and intermittently. We apply z-score normalization at the whole night-level. Then downsample the data to have features and labels each minute, as EEG data is sampled at 100Hz and labels are sampled at 1Hz. We then split the data into subsequences of a fixed size 100. We use a batchsize of 512.

EEG EYE from UC Irvine [53] consists of data measured from one continuous participant tasked with opening and closing their eyes while wearing a headset to measure their EEG data. We apply z-score normalization for the entire sequence, remove outliers (>5 SD away from mean), and split into subsequences of a fixed size 50. We use a batchsize of 128.

D.2. Specific Implementation Details

GRU the GRU $r : \mathbb{R}^d \times \mathbb{Z} \rightarrow \mathbb{R}^C \times \mathbb{Z}$ produces an *output vector* such that the output of $r(x_t, z_{t-1})$ is our model for $h_\theta(x_{1:t})$, and a *hidden state* $z_t \in \mathbb{Z}$ that summarizes $x_{1:t}$. We use a softmax activation on the output vector of the GRU to make it a valid parameterization of $p_\theta(y_t | x_{1:t})$. The GRU has a single hidden layer with a 32 dimension hidden state.

TENOR TENOR uses an additional fully-connected neural network with 10 hidden layers that outputs a $C * C$ -dimensional vector to represent each entry of a flattened \hat{Q}_t . To ensure the output of this network is valid for Def. 1, we reshape the prediction to be $C \times C$, apply a row-wise softmax function, add this to the identity matrix to ensure diagonal dominance, then rescale the rows to be row-stochastic. These operations are all differentiable, ensuring we can optimize this network with standard backpropagation.

VolMinNet and VolMinTime We do a similar parameterization for VolMinNet and VolMinTime, using a set of differentiable weights to represent the entries of \hat{Q}_t rather than a neural network.

Anchor and AnchorTime Patrini et al. [43] show that in practice taking the 97th percentile anchor points rather than the maximum yield better results, so we use that same approach in our experiments. They also describe a two-stage approach: 1) estimate the anchor points after a warmup period 2) use the anchor points to train the classifier with forward corrected loss. We set the warmup period to 25 epochs.

D.3. Experimental Parameters

Given that the learning algorithm only has access to a noisy training dataset and performance is evaluated on a clean test set, a validation set must be drawn from clean test data or by manually cleaning the noisy training dataset which may be impractical. This makes hyperparameter tuning difficult in noisy label learning. As the optimal set of hyperparameters within each could vary for each method, noise type, amount of noise, and dataset, this represents a difficult task. To be fair for our experimental evaluations, we use the same set of hyperparameters for experiment, and only manually set batch size for each dataset.

Each model was trained for 150 epochs using the adam optimizer with default parameters and a learning rate of 0.01.

For VolMinNet, VolMinTime, and TENOR we use adam optimizer with default parameters and a learning rate of 0.01 to optimize each respective \hat{Q}_t -estimation technique. λ was set to $1e - 4$ for VolMinNet and VolMinTime for all experiments, based on what was published previously [33].

D.4. Noise Injection

To the best of our knowledge there are no noisy label time series datasets (i.e.: standardized datasets with both clean and noisy labels) to evaluate our methods. In line with prior experimental approaches, we propose a noise injection strategy which assumes some temporal noise function that can give us a noisy distribution to evaluate from. We deliberately pick a wide variety of noise types, varying the amount and functional form of time-dependent noise, including static noise setting (uniform noise at every time, akin to what baseline methods assume), and class-dependent noise structure Fig. 4.

E. Complete Results

E.1. Forward vs Backward Loss

Here we explain some counter-intuitive results observed when comparing the *backward sequence loss* and *forward sequence loss* in static and temporal noise. We can understand this behaviour by realizing that *backward sequence loss* requires an explicit matrix-inversion which multiplies into your uncorrected loss term. This involves an inverse-determinant term that scales the loss at every time step. Consider the $C = 2$ setting, the magnitude of this term is controlled by the product of the off-diagonal entries - i.e: it approaches ∞ as the noise for each class in Q_t approaches the upper bound of noise 0.5. This is why in Fig. 5, *backward sequence loss* performs particularly poorly in high noise. In the static case, where we average Q_t over time, we bound the inverse-determinant at each time step, therefore controlling these gradients by reducing the effect of any high noise time steps. In the Mixed noise setting in Fig. 5, we increase the noise in one class while decreasing the noise in the other over time, so the off-diagonal entries in Q_t never reach their upper bound at the same time. As a result this again provides a mechanism to control the inverse-determinant.

We provide complete comparisons of *backward sequence loss* and *forward sequence loss* across varying degrees of noise and all temporal noise functions in Fig. 5.

Figure 4: Temporal functions that can be specified using a temporal label noise function $Q(t)$. We present six examples for binary classification task (from top-left clockwise): time independent, exponential decay sinusoidal noise, mixed class-dependent noise, linear decay noise, sigmoid increasing noise. Each plot shows the off-diagonal entries of various parameterized forms of $Q(t)$.

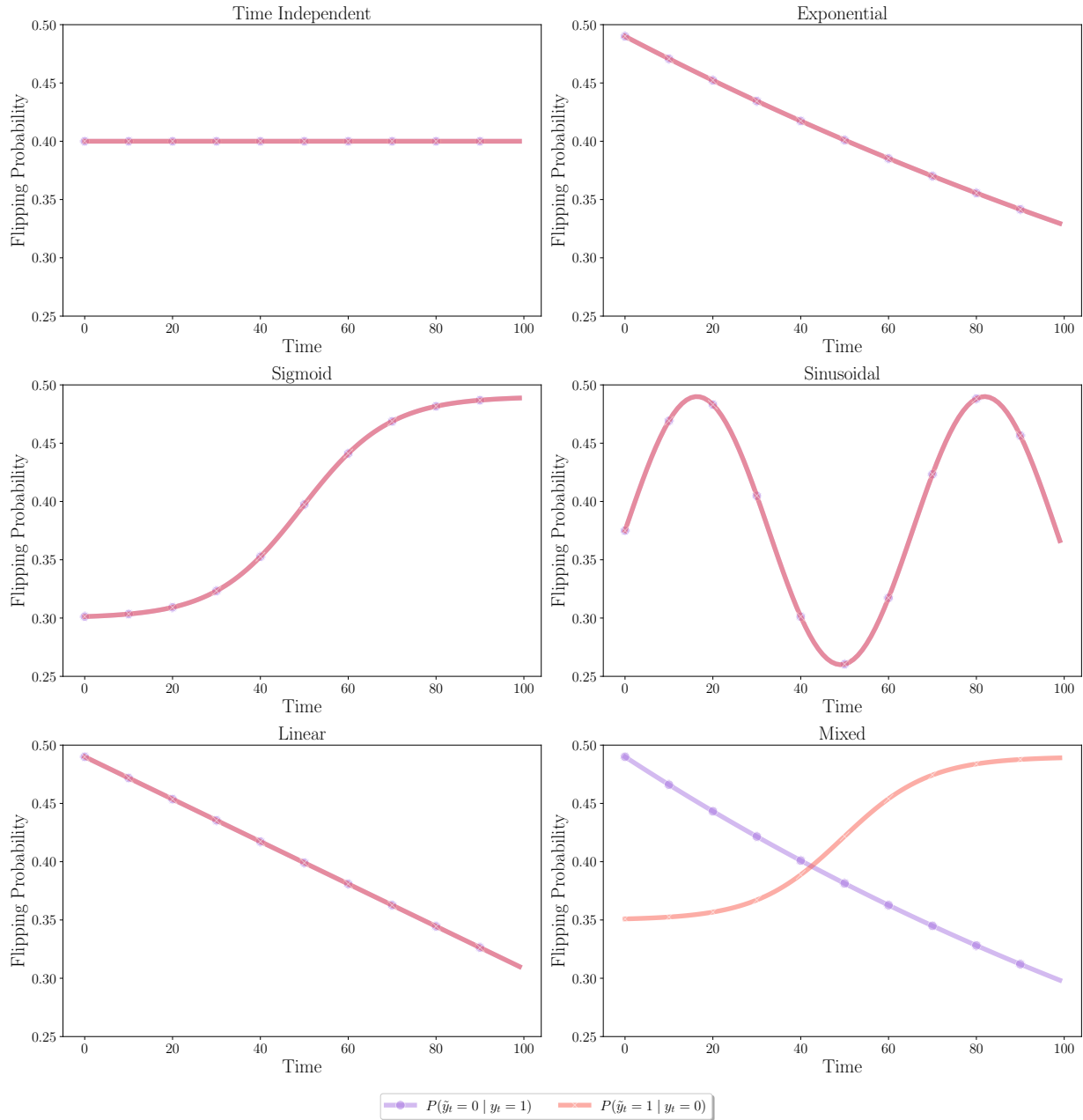
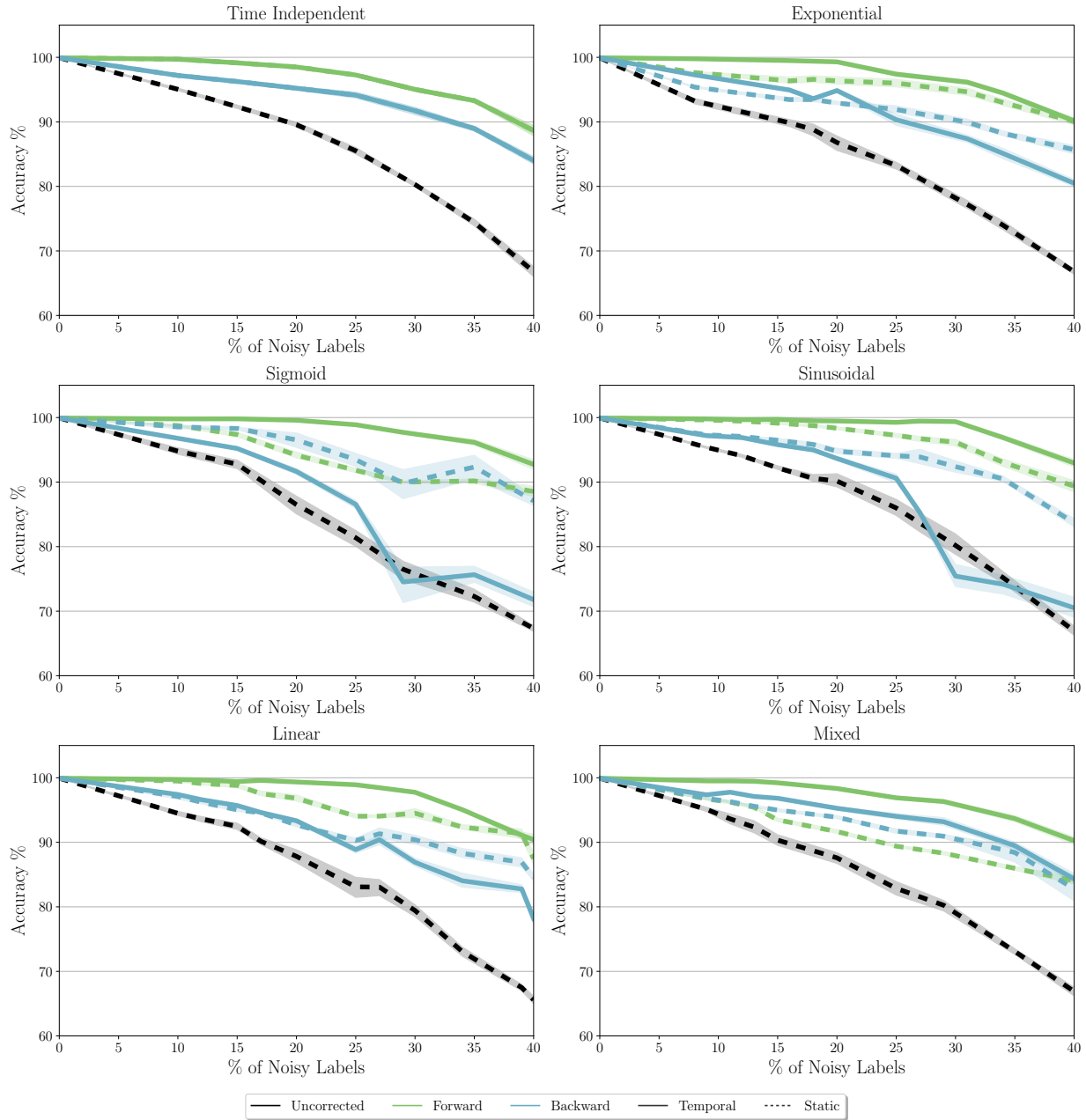


Figure 5: Comparing performance of models trained with *backward sequence loss* and *forward sequence loss* on *synth* with varying degrees of temporal label noise using either the true temporal noise function (Temporal) or the average temporal noise function (Static). Error bars are st. dev. over 10 runs.



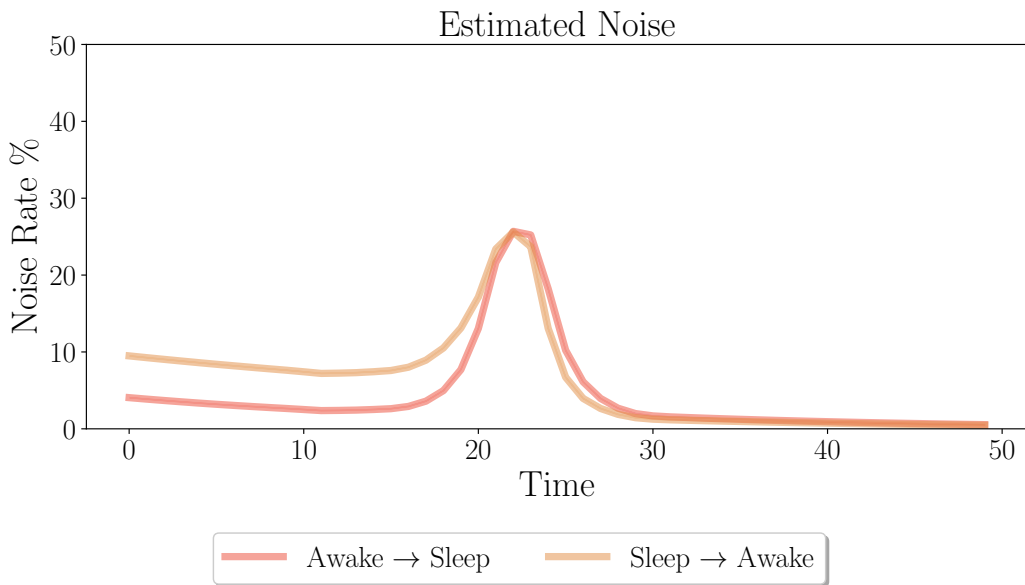
E.2. Real Temporal Label Noise

Prior work in the static noisy label literature typically aim to demonstrate the effectiveness of their methods on a real world noisy dataset, where the noise function is not imposed by the researcher. The primary dataset used is the `Clothing1M` dataset [74]. Despite containing real label noise, `Clothing1M` is inapplicable in our setting: it is not sequential data and each instance has only one label. In the spirit of evaluating TENOR on real-world noisy labels, we discovered and experimented with `extrasensory`, a noisy-labelled time series dataset [64]. `extrasensory` includes human activity data from smartphones and smartwatches collected from 60 users spread across 300,000 minutes of measurements. In contrast to `har` and `har70` (datasets originally used in our paper), `extrasensory` has no expert-labelled annotations, all the labels are user-provided and therefore are highly noisy. Users often misreport falling asleep and waking up, so we expect particularly high label noise during sleep/awake transitions

In order to identify the label noise in this sequential data, we partition and center the dataset from all users around sleep/awake transition periods. That is, for a fixed length window of 50, sleep/awake transitions occur around the $t = 25$ point. We then train our TENOR objective with the same model architecture and hyperparameters as above to classify sleep and awake over time. Since there are no 'clean' labels, we demonstrate that TENOR successfully identifies an interpretable temporal noise function.

In Fig. 6, we see TENOR predicts there exists higher label noise near sleep/awake transitions (around $t = 25$). We hope our work also encourages the community to seek further sources of real temporal noise.

Figure 6: TENOR-estimated \hat{Q}_t for `extrasensory`. Error bars are st. dev. over 10 runs.



E.3. Accuracy over Varying Degrees Noise

E.4. MAE over Varying Degrees Noise

Figure 7: Comparison of clean test set Accuracy (%) for `synth` across varying degrees of temporal label noise comparing all methods. Error bars are st. dev. over 10 runs.

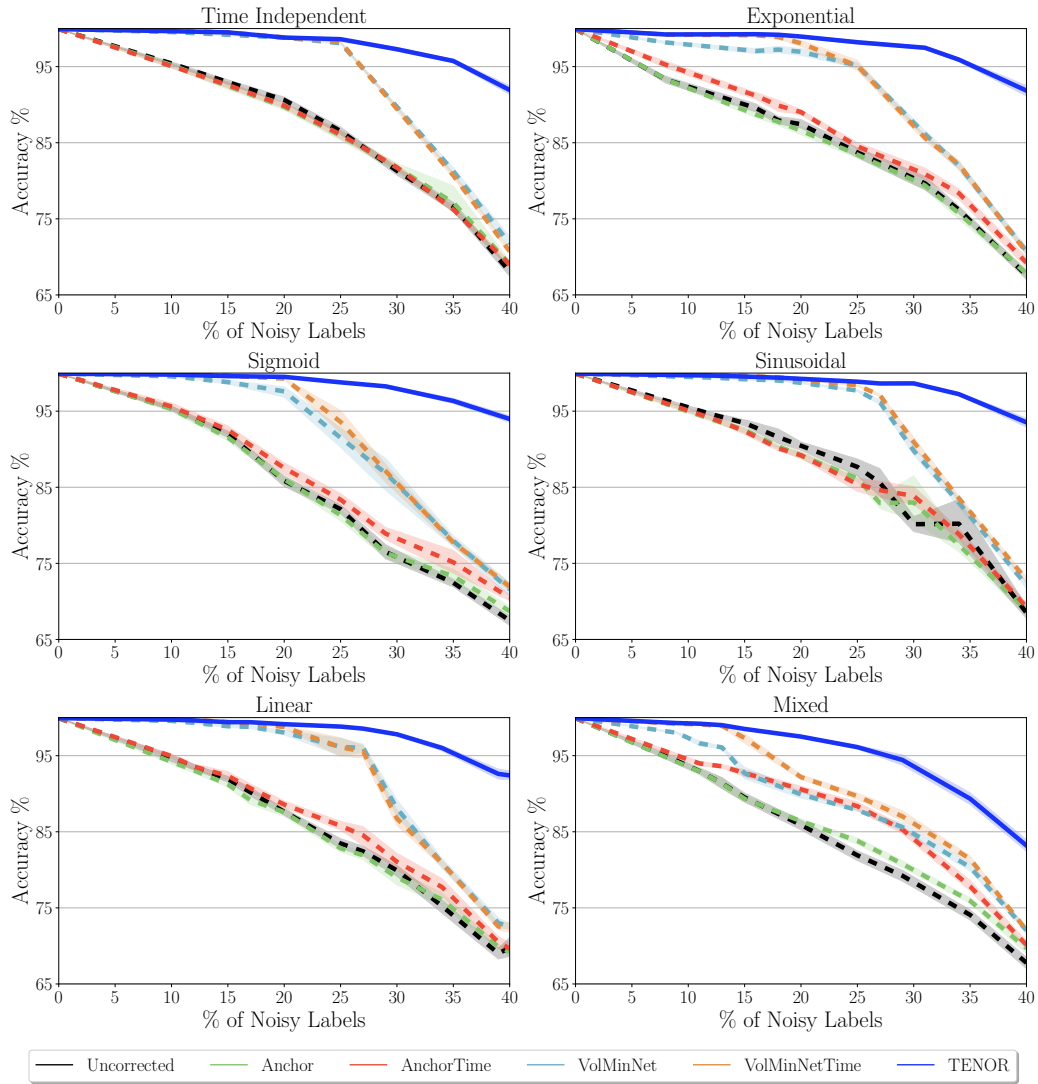


Figure 8: Comparison of clean test set Accuracy (%) for `har` across varying degrees of temporal label noise comparing all methods. Error bars are st. dev. over 10 runs.

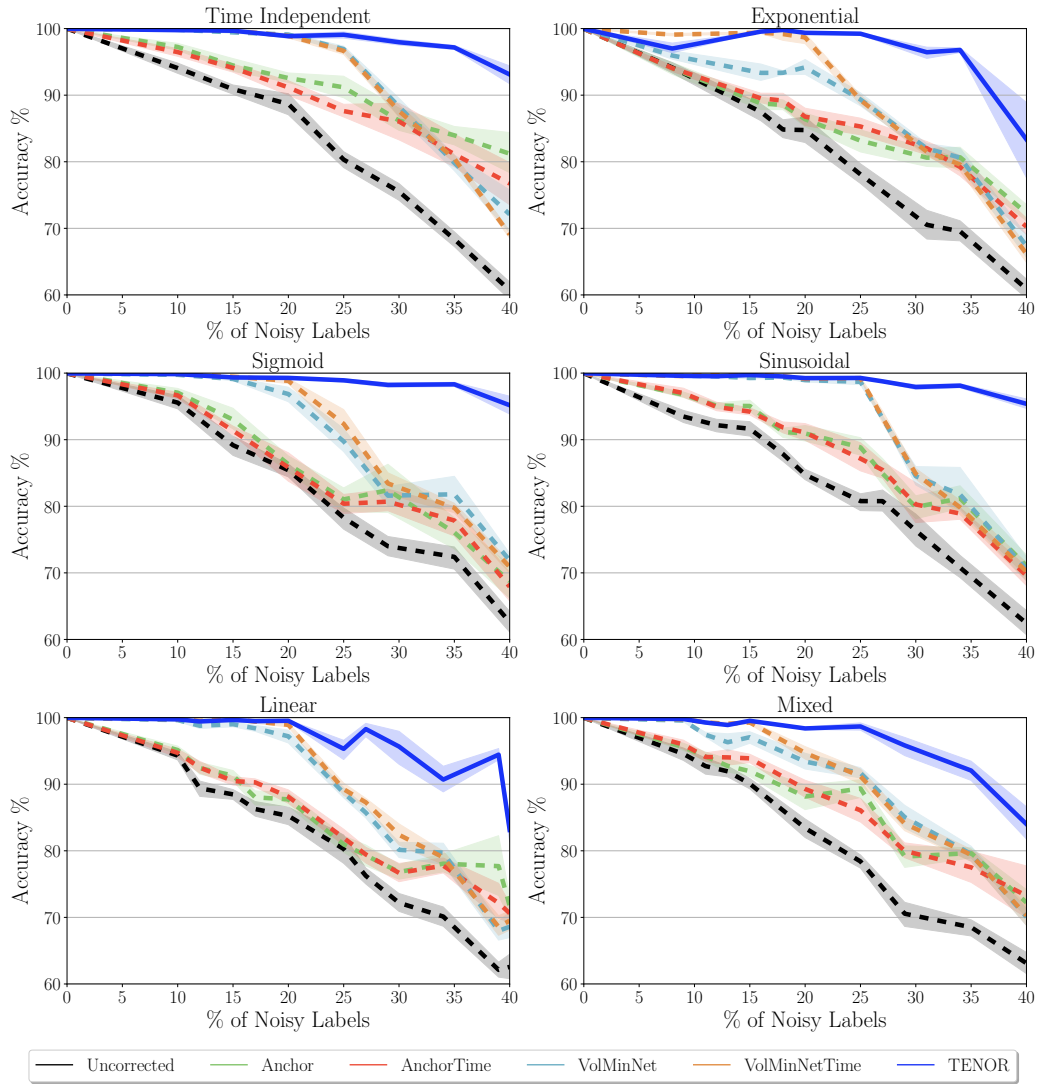


Figure 9: Comparison of clean test set Accuracy (%) for `har70` across varying degrees of temporal label noise comparing all methods. Error bars are st. dev. over 10 runs.

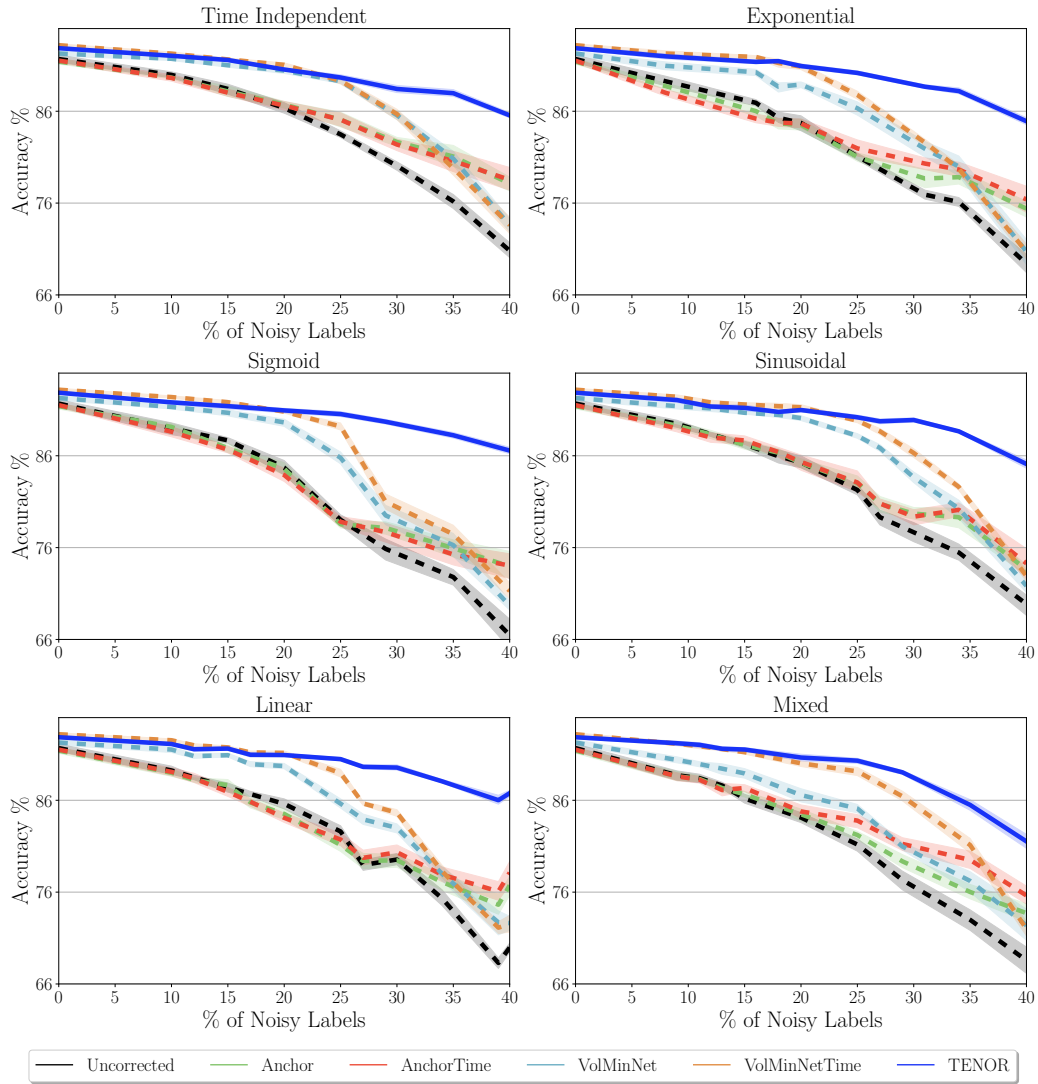


Figure 10: Comparison of clean test set Accuracy (%) for `eeg_sleep` across varying degrees of temporal label noise comparing all methods. Error bars are st. dev. over 10 runs.

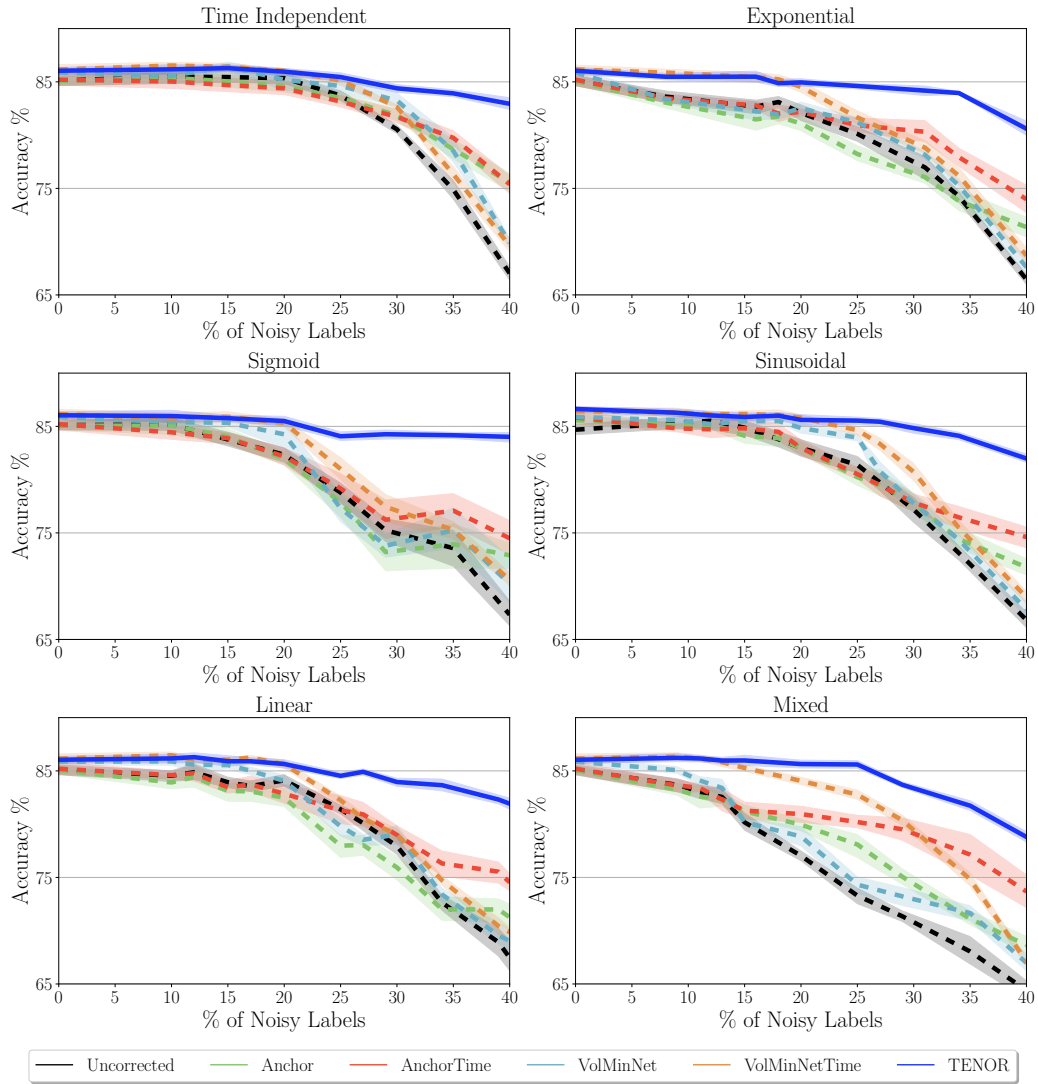


Figure 11: Comparison of clean test set Accuracy (%) for eeg_eye across varying degrees of temporal label noise comparing all methods. Error bars are st. dev. over 10 runs.

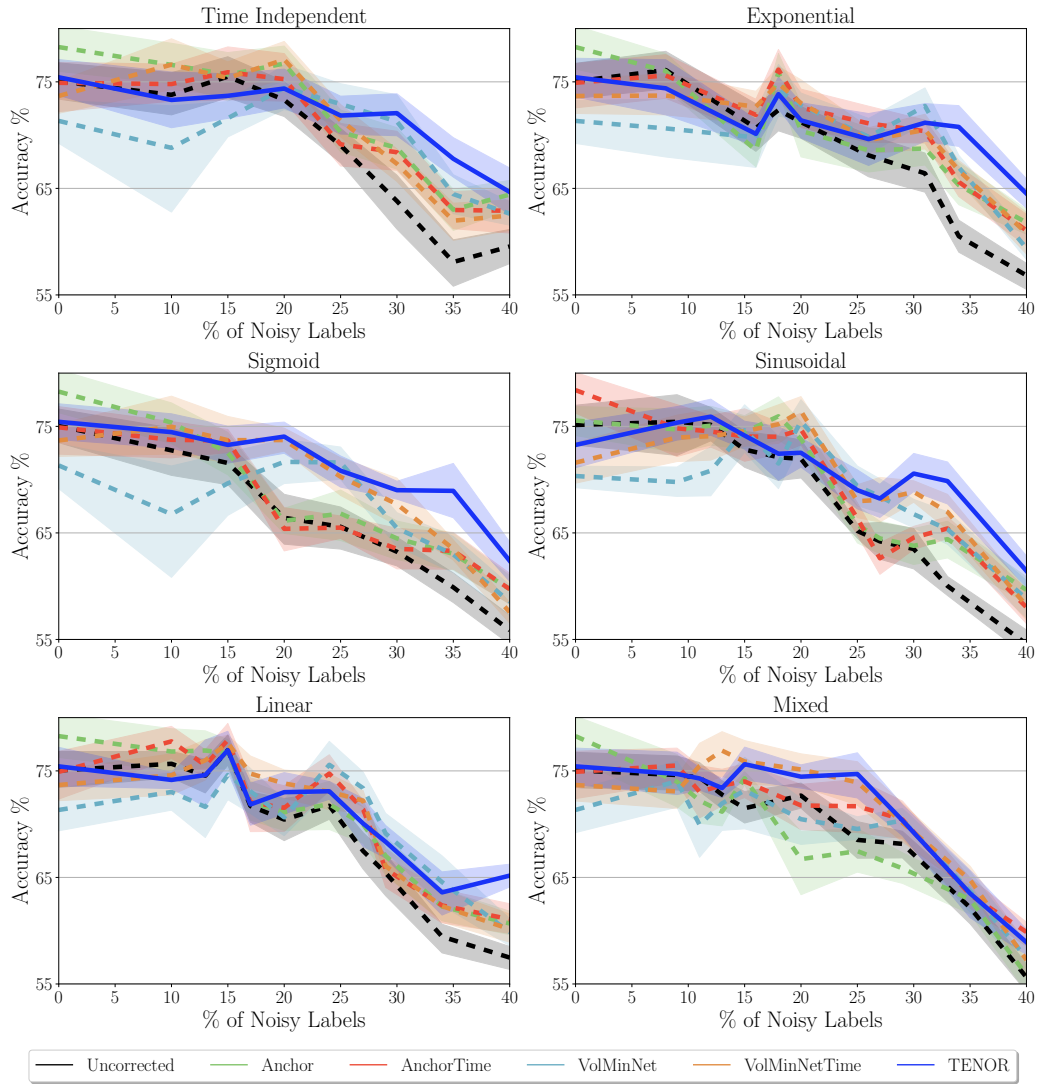


Figure 12: Comparison of noisy function reconstruction Mean Absolute Error (MAE) for `synth` across varying degrees of temporal label noise comparing all methods. Error bars are st. dev. over 10 runs.

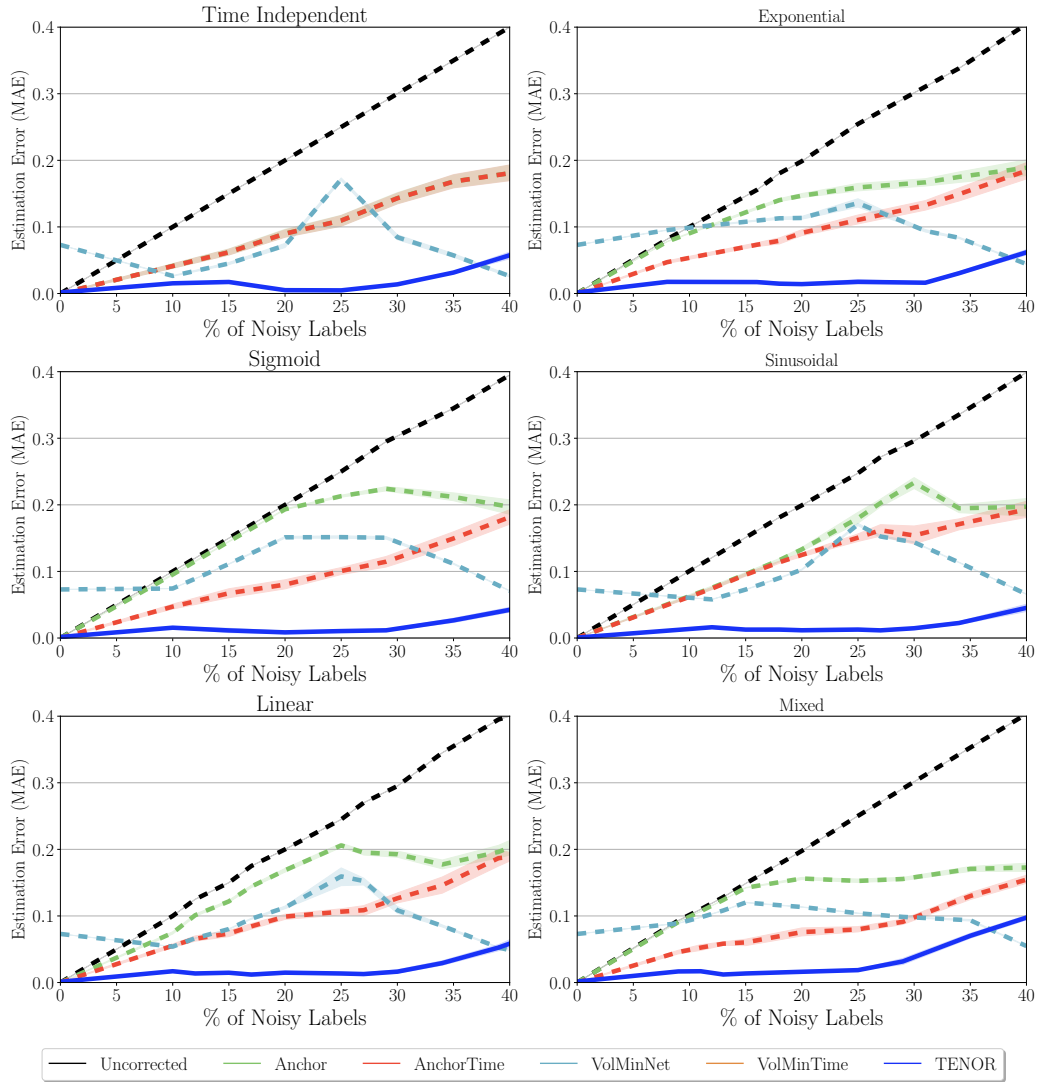


Figure 13: Comparison of noisy function reconstruction Mean Absolute Error (MAE) for har across varying degrees of temporal label noise comparing all methods. Error bars are st. dev. over 10 runs.

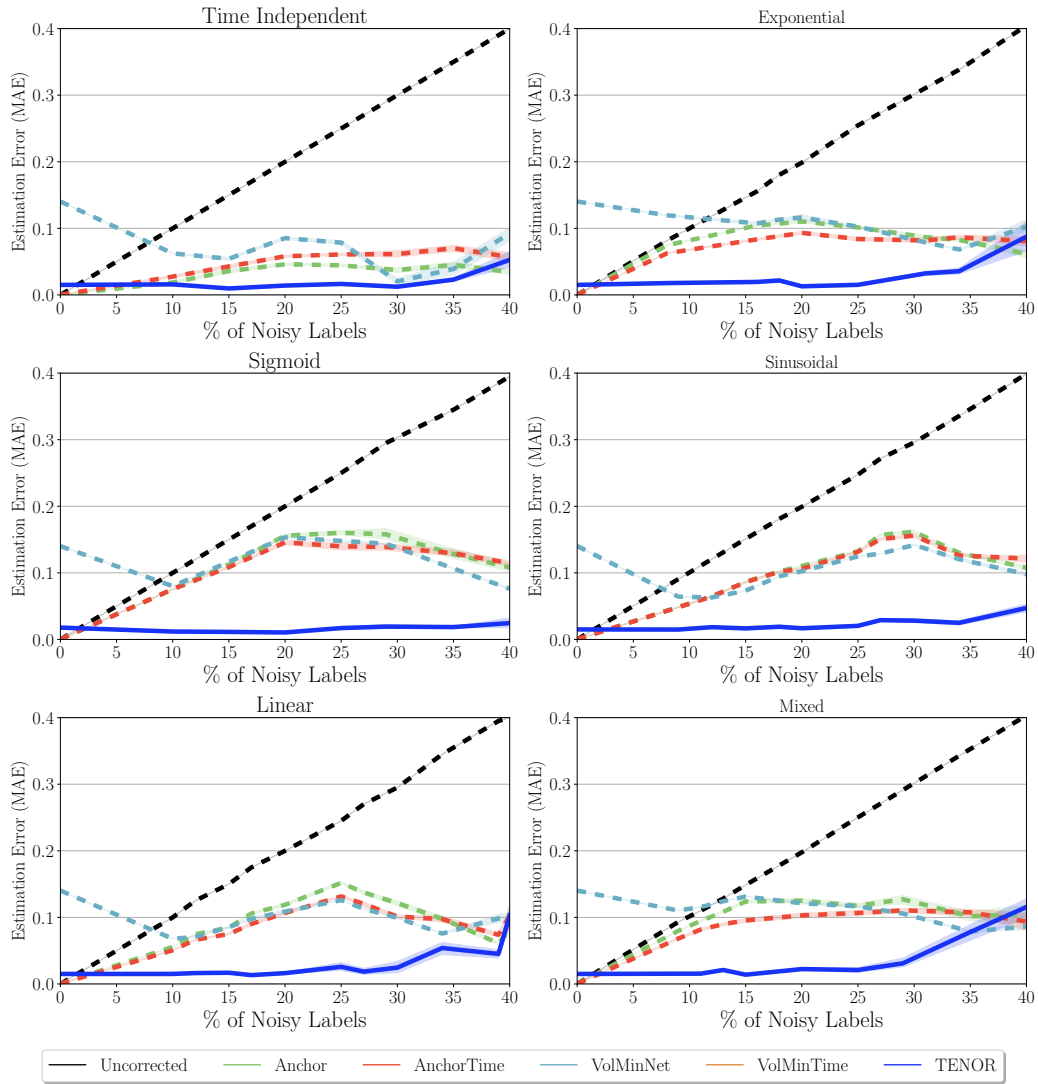


Figure 14: Comparison of noisy function reconstruction Mean Absolute Error (MAE) for `har70` across varying degrees of temporal label noise comparing all methods. Error bars are st. dev. over 10 runs.

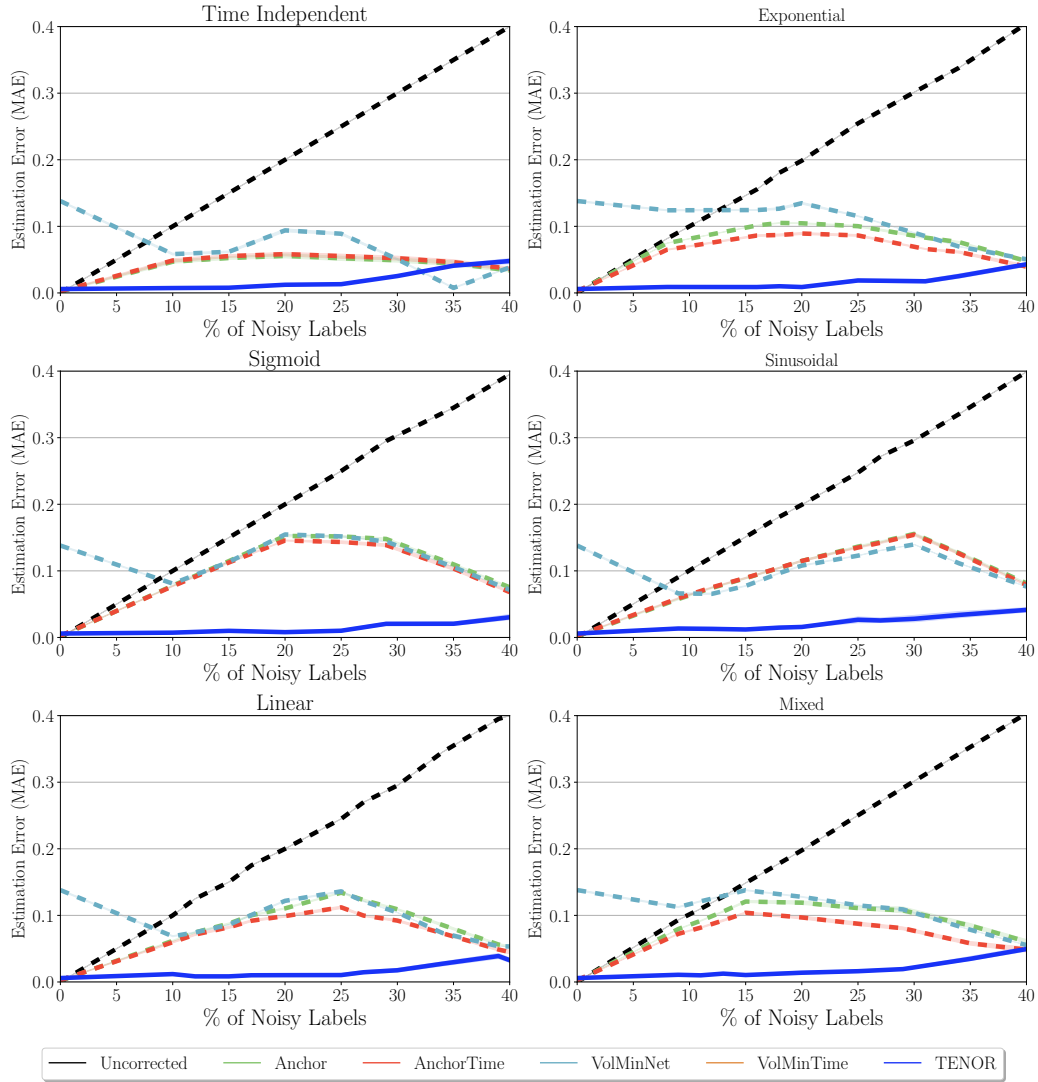


Figure 15: Comparison of noisy function reconstruction Mean Absolute Error (MAE) for `eeg_sleep` across varying degrees of temporal label noise comparing all methods. Error bars are st. dev. over 10 runs.

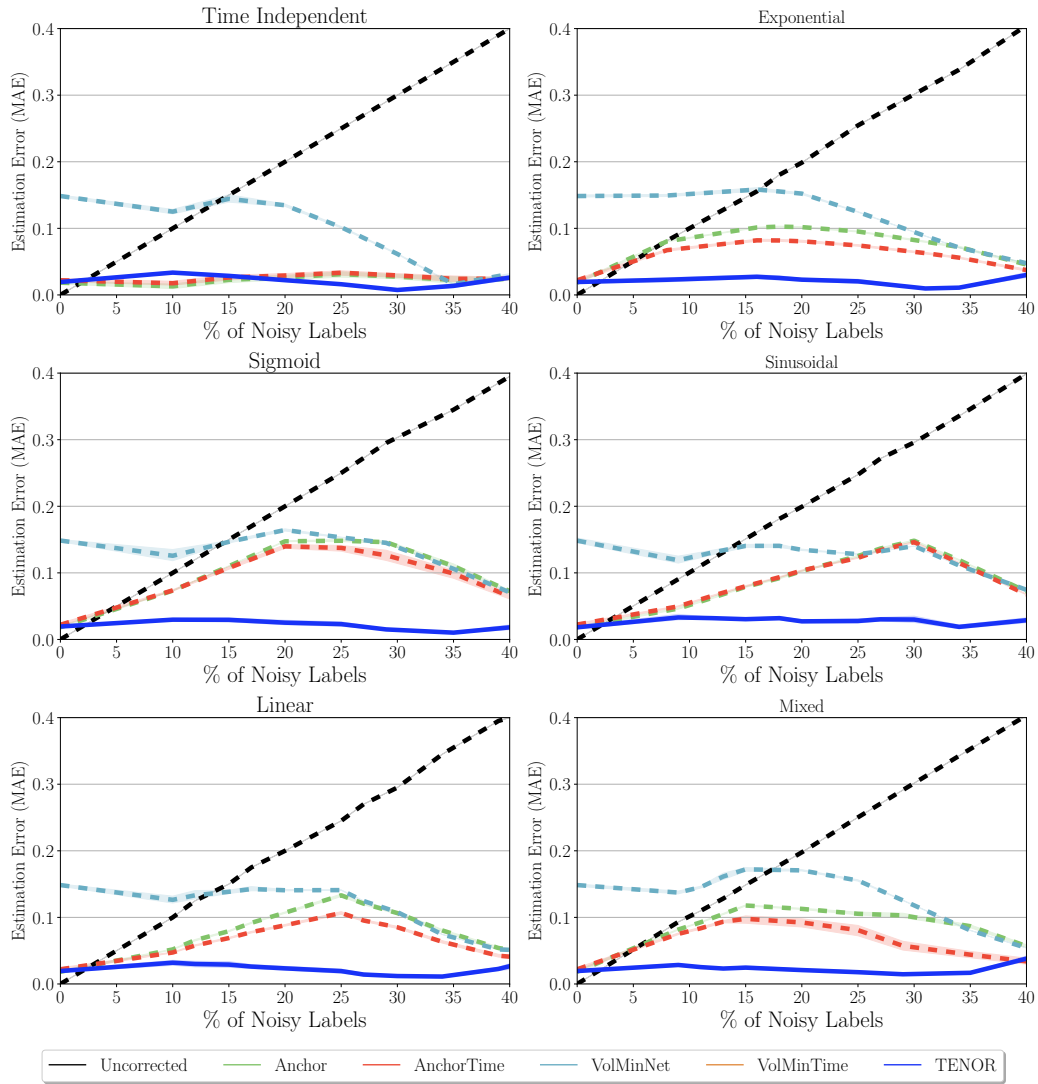
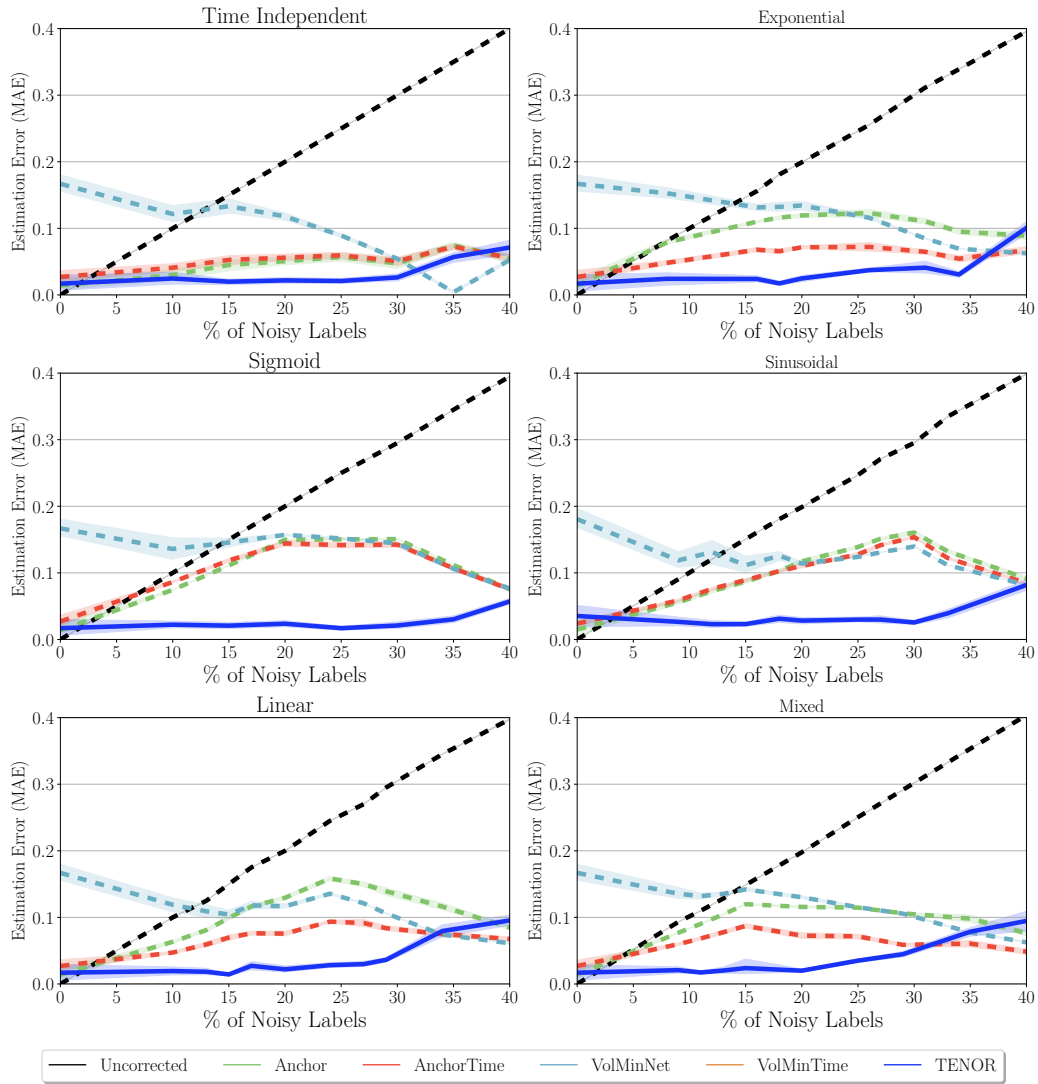


Figure 16: Comparison of noisy function reconstruction Mean Absolute Error (MAE) for `eeg_eye` across varying degrees of temporal label noise comparing all methods. Error bars are st. dev. over 10 runs.



E.5. Choice of Loss and Optimization Strategy

In our experiments we have slightly different loss terms for TENOR and VoMinTime, with the former penalizing the Frobenius norm and the latter penalizing the LogDet. We also use a special augmentation strategy for TENOR, the augmented Lagrangian method. In order to show that these changes are not what is leading to differences in performance, we compare TENOR to versions of VoMinTime using both types of losses and the augmented Lagrangian optimization method (VoMinTime-AL).

Figure 17: Comparison of clean test set Accuracy (%) for synth across varying degrees of temporal label noise comparing loss functions for VoMinTime. Error bars are st. dev. over 10 runs.

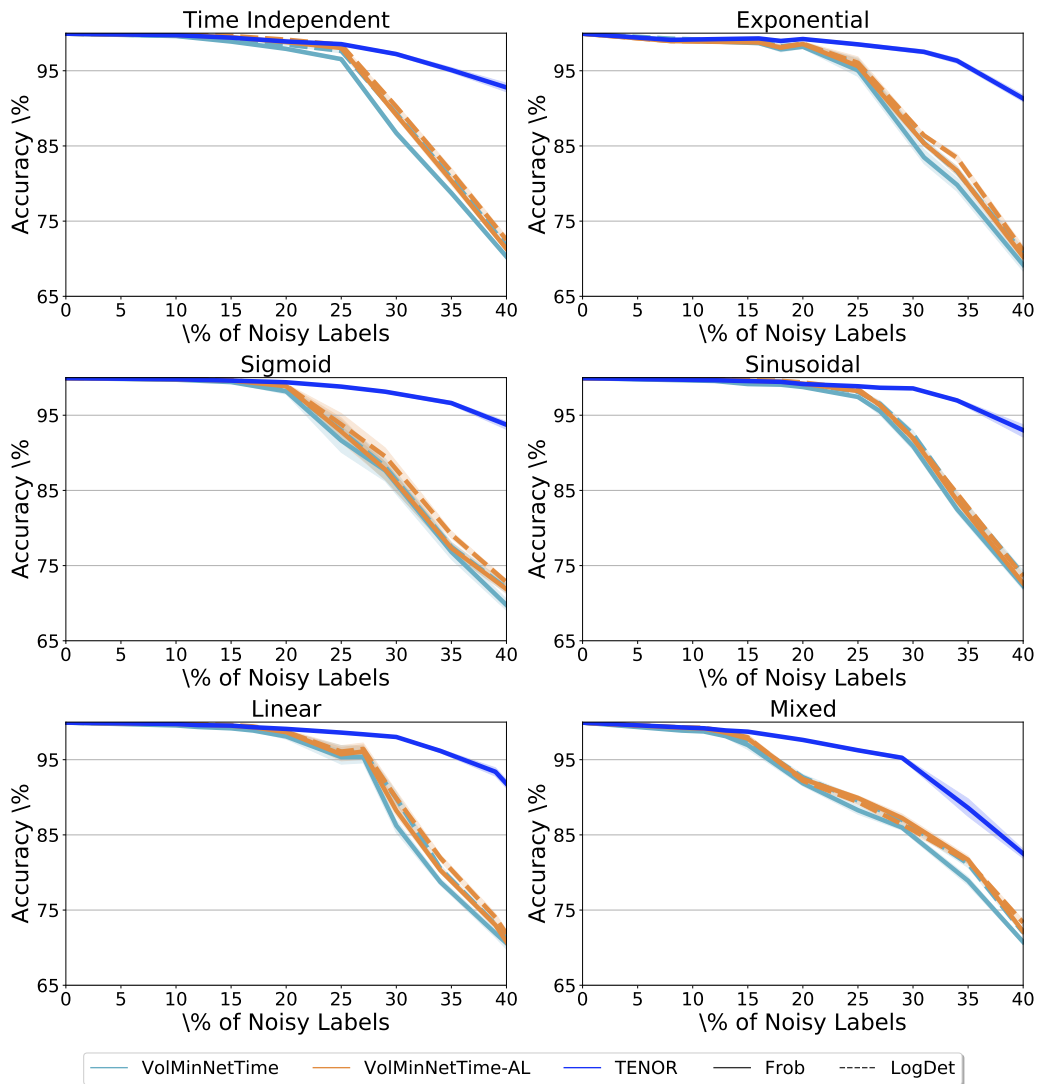
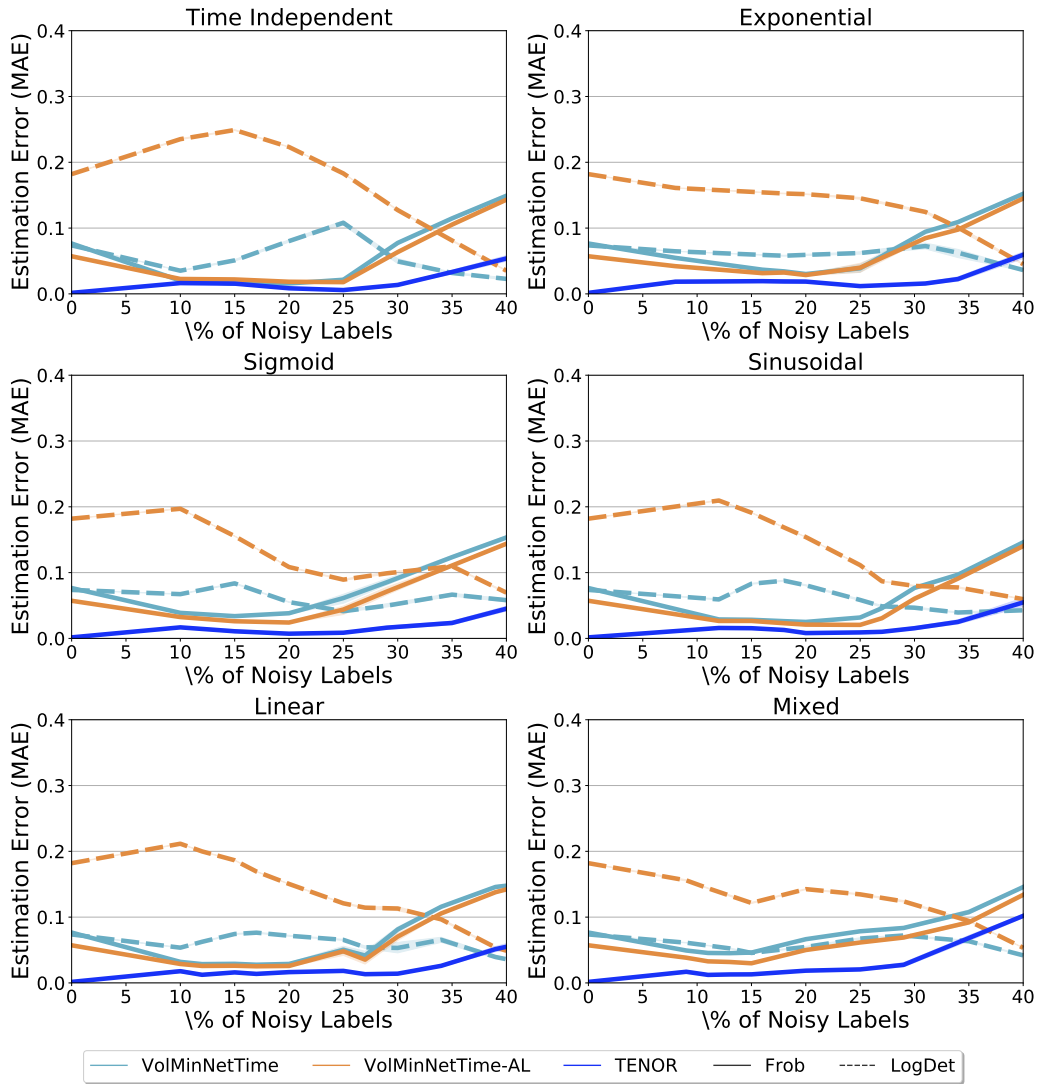


Figure 18: Comparison of noisy function reconstruction Mean Absolute Error (MAE) for `synth` across varying degrees of temporal label noise comparing loss functions for VoIMinTime. Error bars are st. dev. over 10 runs.



E.6. Class Dependent and Class Independent

E.7. Multiclass Classification

Table 5: Comparison of clean test-set Accuracy (%) and MAE of all methods on Class Independent and Class Dependent sinusoidal label noise for a fixed degree of label noise (30%) on *har*. Dashed line separates *Static* and *Temporal* methods.

		Class Independent		Class Dependent	
		Accuracy \uparrow	MAE \downarrow	Accuracy \uparrow	MAE \downarrow
Static	Uncorrected	76.0 \pm 5.1	–	76.4 \pm 3.1	–
	Anchor	82.0 \pm 3.6	0.15 \pm 0.014	84.2 \pm 2.2	0.13 \pm 0.012
	VolMinNet	86.5 \pm 6.0	0.13 \pm 0.009	92.6 \pm 1.9	0.12 \pm 0.012
Temporal	AnchorTime	81.5 \pm 4.3	0.14 \pm 0.013	84.1 \pm 2.3	0.13 \pm 0.010
	VolMinTime	86.0 \pm 5.7	0.10 \pm 0.015	91.5 \pm 2.1	0.08 \pm 0.004
	TENOR	98.3 \pm 0.6	0.03 \pm 0.005	98.4 \pm 0.7	0.02 \pm 0.005

Figure 19: Comparison of clean test set Accuracy (%) for *synth* across varying degrees of temporal label noise comparing all methods for 3-class classification. Error bars are st. dev. over 10 runs.

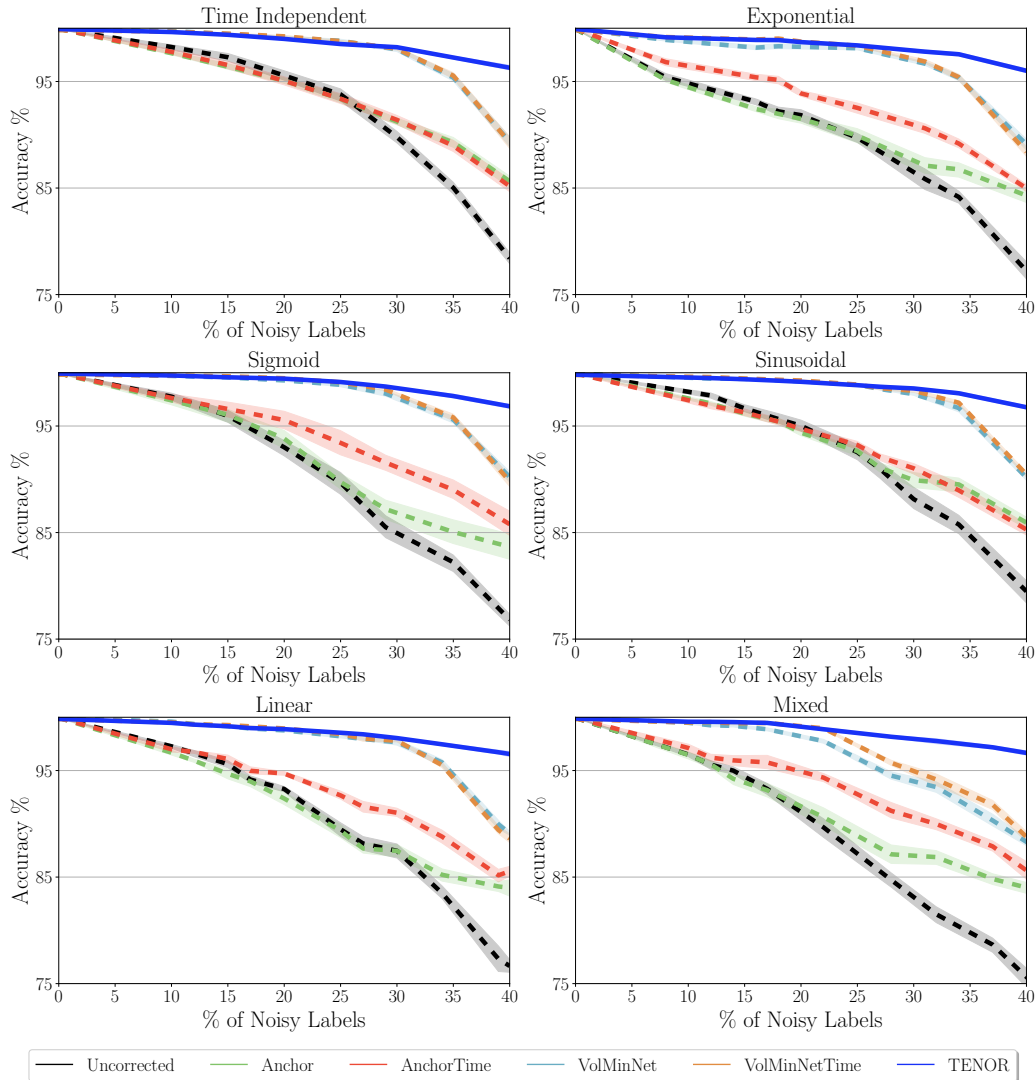


Figure 20: Comparison of noisy function reconstruction Mean Absolute Error (MAE) for `synth` across varying degrees of temporal label noise comparing all methods for 3-class classification. Error bars are st. dev. over 10 runs.

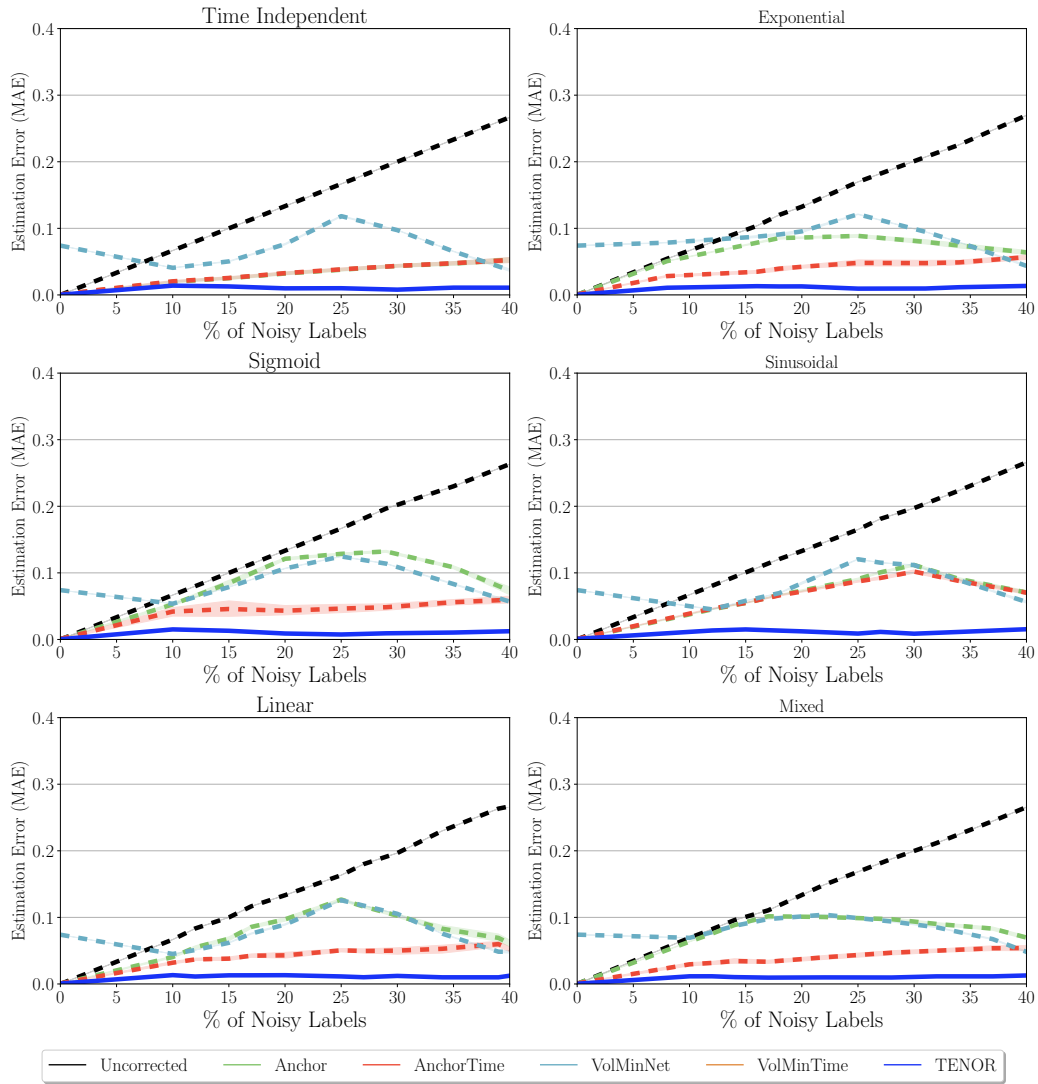


Figure 21: Comparison of clean test set Accuracy (%) for `eeg_sleep` across varying degrees of temporal label noise comparing all methods for 3-class classification. Error bars are st. dev. over 10 runs.

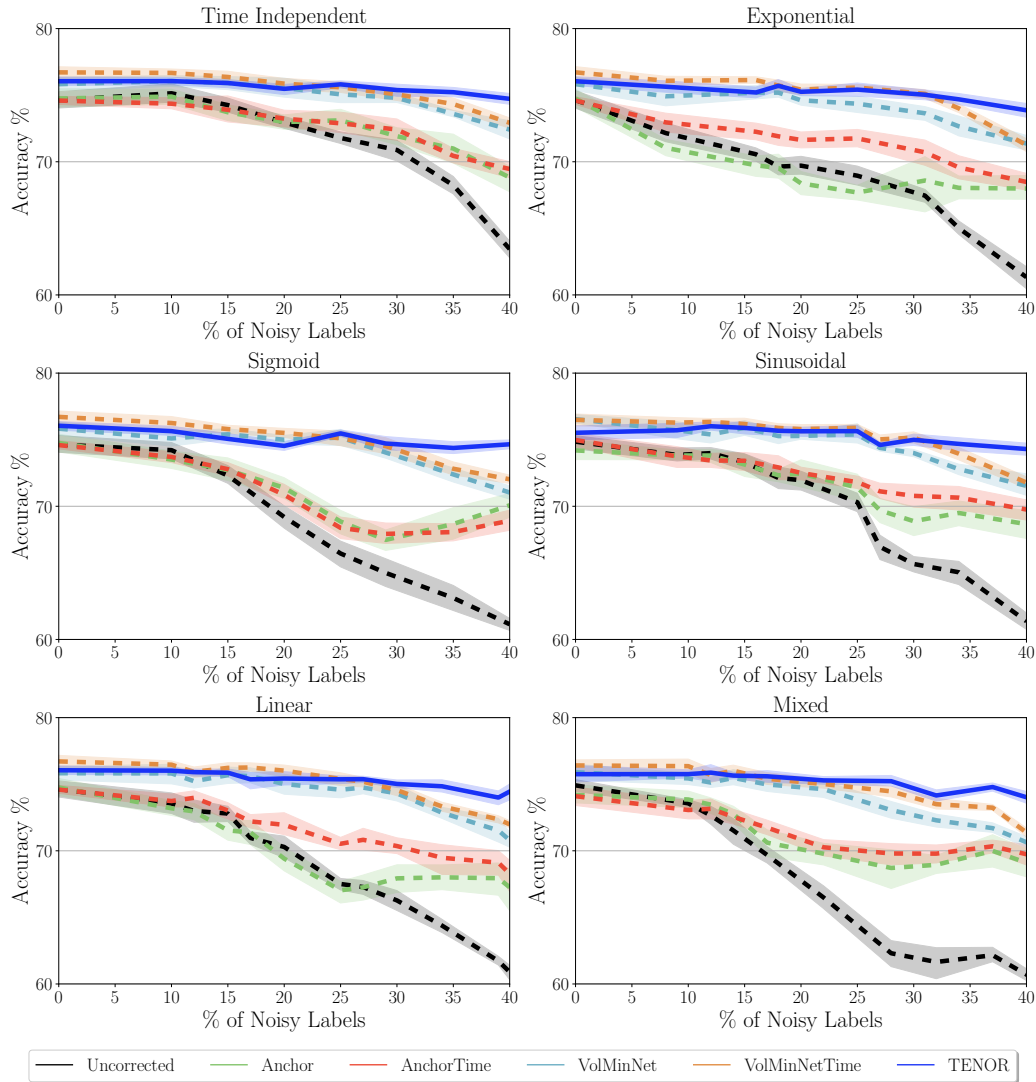


Figure 22: Comparison of noisy function reconstruction Mean Absolute Error (MAE) for `eeg_sleep` across varying degrees of temporal label noise comparing all methods for 3-class classification. Error bars are st. dev. over 10 runs.

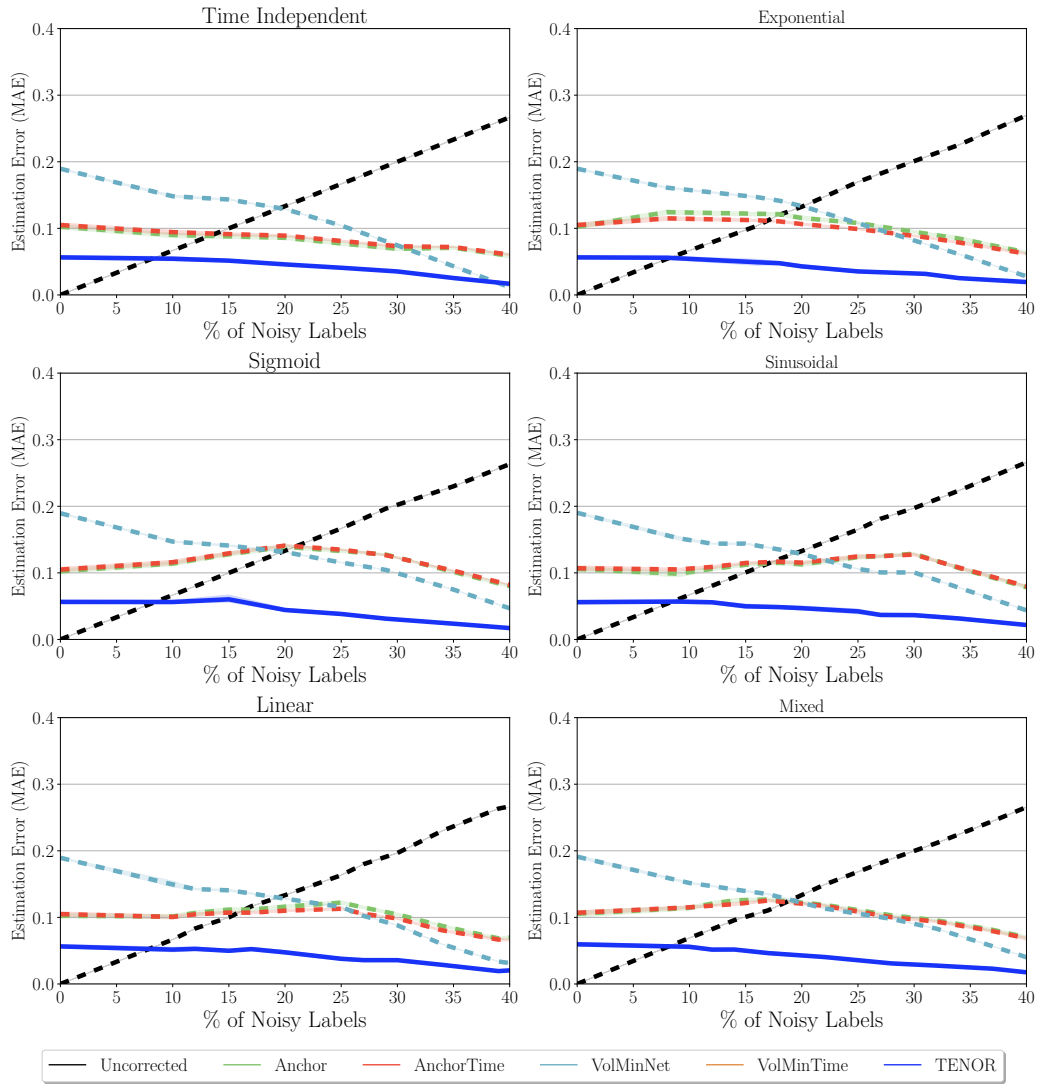


Figure 23: Comparison of clean test set Accuracy (%) for h_{ar} across varying degrees of temporal label noise comparing all methods for 4-class classification. Error bars are st. dev. over 10 runs.

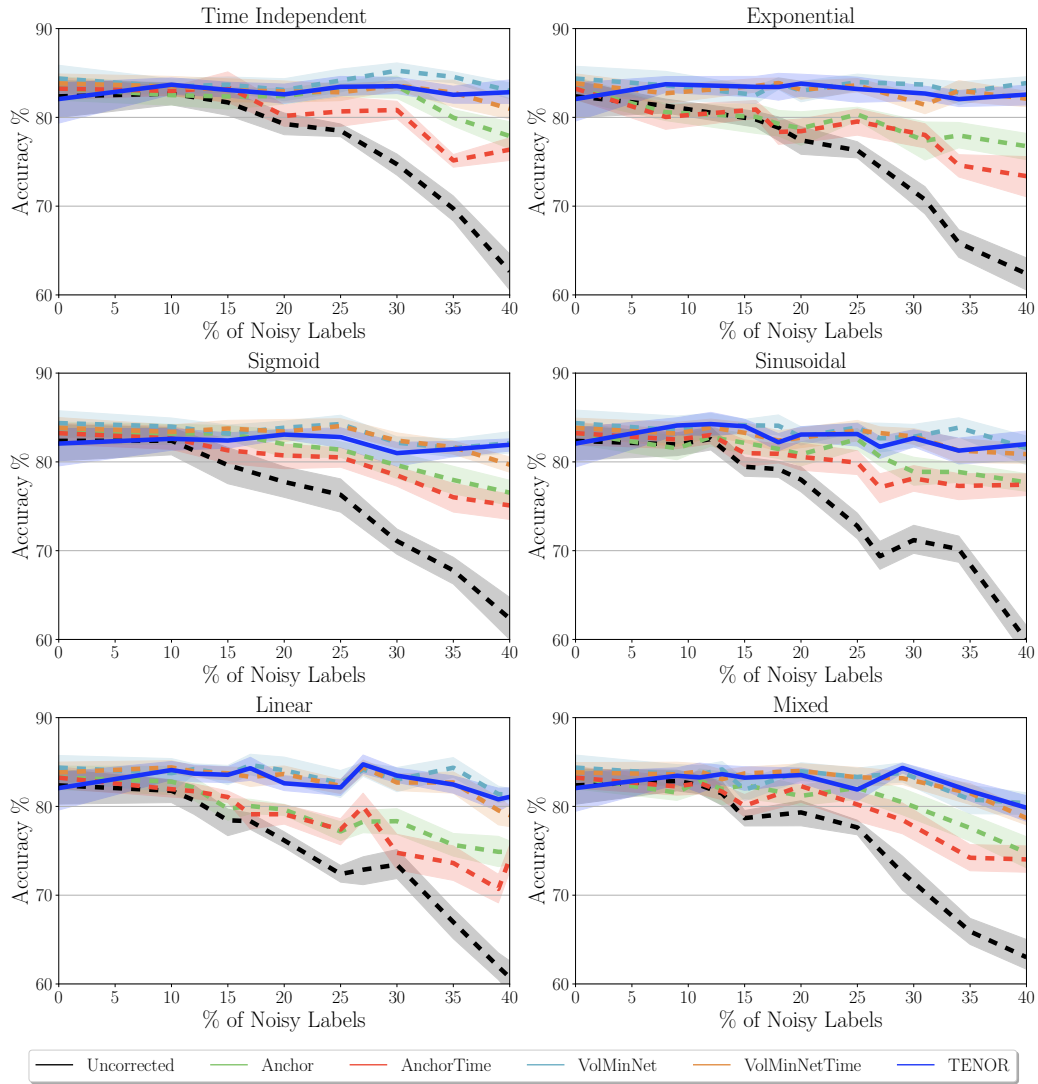


Figure 24: Comparison of noisy function reconstruction Mean Absolute Error (MAE) for har across varying degrees of temporal label noise comparing all methods for 4-class classification. Error bars are st. dev. over 10 runs.

